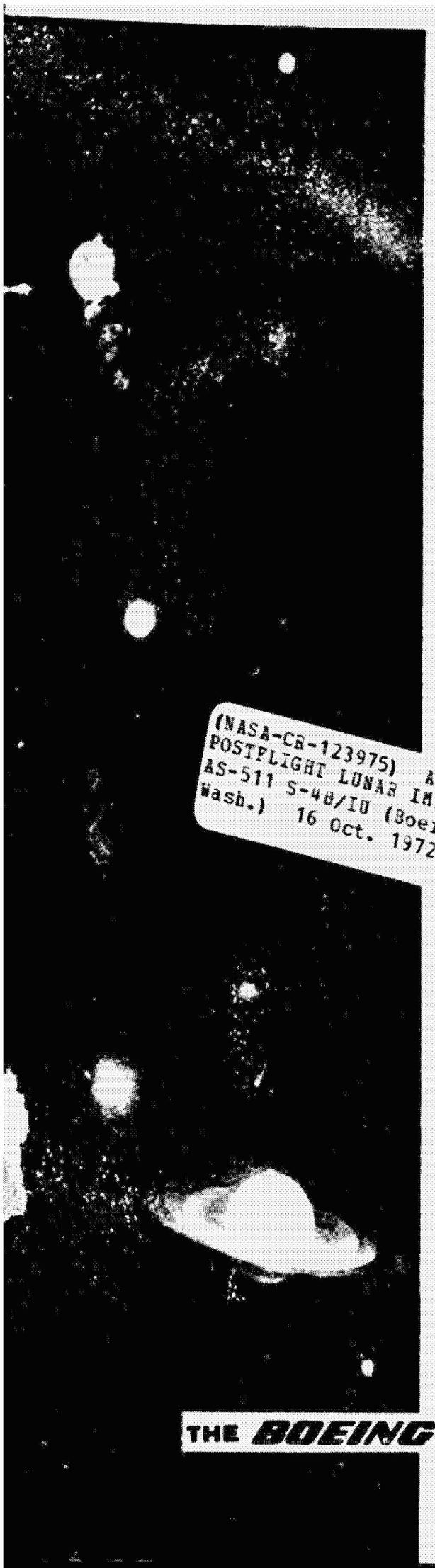

D5-15814-3

APOLLO/SATURN V POSTFLIGHT LUNAR IMPACT TRAJECTORY - AS-511 S-IVB/IU

OCTOBER 16, 1972

THE BOEING COMPANY - SPACE DIVISION

DOCUMENT NO. D5-15814-3

TITLE APOLLO/SATURN V POSTFLIGHT LUNAR IMPACT TRAJECTORY - AS-511 S-IVB/IU

MODEL NO. SATURN V CONTRACT NO. NAS8-5608, EXHIBIT CC, SCHEDULE II, PART VIII, TASK 5.1.8, LINE ITEM 60F (PART B)

TRACKING AND FLIGHT RECONSTRUCTION
G. T. PINSON

OCTOBER 16, 1972

W. B. MORGAN, MANAGER
FLIGHT TECHNOLOGY

ISSUE NO. ISSUED TO

THE BOEING COMPANY SPACE DIVISION LAUNCH SYSTEMS BRANCH

ABSTRACT AND LIST OF KEY WORDS

This document presents the postflight trajectory for the Apollo/Saturn V AS-511 spent S-IVB/IU stage from CSM separation to lunar impact. The lunar impact coordinates and conditions are included. Some combinations of small S-IVB/IU stage related forces are hypothesized to account for a significant angular momentum increase and small translational perturbations. Trajectory dependent parameters in geocentric and selenocentric inertial coordinates (PACSS4, reference epoch at mean nearest Besselian year) are listed at selected time points from Command Service Module separation to lunar impact.

Data relating to the tracking residuals (observed minus model calculated (O-C)) are also given for the best-estimate trajectory.

Apollo/Saturn V
S-IVB/IU Spent Stage
AS-511
Postflight Trajectory
Lunar Impact Conditions
Apollo 16
BET

CONTENTS

REFERENCES

1. NASA Document MPR-SAT-FE-72-1, "Saturn V Launch Vehicle Flight Evaluation Report - AS-511 Apollo 16 Mission," June 19, 1972.

2. GSFC Memorandum, "Apollo 16 STDN Metric Tracking Performance (Preliminary)," May 1972.

3. Lockheed Missiles and Space Company Document (LMSC/HREC D162559) TM54/30-235, "LID User's Manual," September 1970.

4. NASA Document SE-008-001-1, "Project Apollo Coordinate System Standards," June 1965.

5. NASA Technical Report 32-1527, "Mathematical Formulation of the Double Precision Orbit Determination Program (DPODP)," May 15, 1971.

6. "An Introduction to Optimal Estimation," Paul B. Liebelt, Addison-Wesley Publishing Company, Copyright 1967.

ACKNOWLEDGEMENT

The analyses presented in this document were conducted under the technical direction of R. McCurdy by the following Saturn Engineering personnel:

TRACKING AND FLIGHT RECONSTRUCTION

R. Bono
J. Burgen
J. Butler
G. Engels
T. Galbraith
J. Jaap
P. Johnson
D. McKellar

BOEING COMPUTER SERVICES

C. Dorries
R. Simmons

Questions concerning the information presented should be directed to the technical supervisor of this analysis:

G. T. Pinson, JC-40
The Boeing Company
Huntsville, Alabama

ILLUSTRATIONS

TABLES

GLOSSARY OF TERMS

TERM	DEFINITION
Docking Maneuver	Command and Service Module attachment to the Lunar Module for subsequent ejection of the CSM/LM from the S-IVB/IU.
Impact Maneuvers	The S-IVB/IU APS burn maneuvers to accomplish lunar targeting of the spent S-IVB/IU stage.
Initial State	A twelve element vector containing, in order, the initial position, initial velocity, non-gravitational acceleration biases, and non-gravitational acceleration scale factors.
Passive Thermal Control Maneuver	The maneuver which starts and maintains rotation of the spent S-IVB/IU stage about the center of mass to prevent differential solar heating.
Range	Line-of-sight distance between the vehicle and a tracking station.
Range Rate	Time rate of change of range.
Safing Maneuvers	The APS Evasive Burn, CVS Vent, and LOX Dump maneuvers of the spent S-IVB/IU stage to separate it from the CSM/LM and to prepare it for lunar targeting.
Tracking Data Residual	Difference between observed and calculated values of a tracking parameter, e.g., range rate.
Trajectory Segment	A portion of a composite trajectory determined from tracking data over a particular time arc which may be propagated by the model equations prior to or following the data arc.

GLOSSARY OF TERMS (Continued)

TERM	DEFINITION
Timebase 8	A time reference established by the LVDC following an inhibit removal by ground command. This time reference follows the docking maneuvers and preceeds the safing maneuvers.
$\vec{h}$,h	Angular momentum vector, angular momentum
θ	Angle between angular momentum vector and spin vector
$\vec{\dot{\phi}}$,$\dot{\phi}$	Spin vector, spin rate
$\vec{\dot{\psi}}$,$\dot{\psi}$	Precession vector, precession rate
$\vec{\omega}$,ω	Angular rate vector, angular rate

LIST OF ABBREVIATIONS

ABBREVIATION	DEFINITION
ACN3	Ascension 30' STDN USB
APS	Auxiliary Propulsion System
BDA3	Bermuda 30' STDN USB
BDQC	Bermuda C-Band Radar
BET	Best-Estimate Trajectory and Impact Point
CPH	Cycles Per Hour
CSM	Command and Service Module
CRO3	Carnarvon 30' STDN USB
CVS	Continuous Vent System
DSN	Deep Space Network
ETC3	Greenbelt Experimental Test Center 30' STDN USB
GDS8	Goldstone 85' STDN USB
GDSW	Goldstone 85' DSN USB
GMT	Greenwich Mean Time
GWM3	Guam 30' STDN USB
GSFC	Goddard Space Flight Center
HAW3	Hawaii 30' STDN USB
HSKW	Tidbinbilla 85' DSN USB
IS	Impact Point Derived From Seismic Data
IU	Instrument Unit
JPL	Jet Propulsion Laboratory
LID	Lunar Impact Determination

LIST OF ABBREVIATIONS (Continued)

ABBREVIATION	DEFINITION
LM	Lunar Module
LOX	Liquid Oxygen
LV	Launch Vehicle
LVDC	Launch Vehicle Digital Computer
MADW	Madrid 85' DSN USB
MIL3	Merritt Island 30' STDN USB
MILC	Merritt Island C-Band Radar
MNBY	Mean Nearest Besselian Year
MSC	Manned Spacecraft Center
MSFN	Manned Space Flight Network
PACSS	Project Apollo Coordinate System Standard
PTC	Passive Thermal Control
STDN	Spaceflight Tracking and Data Network
USB	Unified S-Band

SOURCE DATA PAGE

The following listed government-furnished documentation was used in the preparation of this document:

Exhibit FF Line Item Number	GFD Title	Date Received
S&E-AERO-17	Tracking and Communications Network Specification	2/14/72
S&E-AERO-73	Operational Trajectory for Saturn V Vehicles	2/14/72
S&E-AERO-104	S-IVB Stage Predicted Nominal Tracking Coverages	2/14/72
S&E-AERO-105	Real-Time Predicted Propulsion and Attitude Data and Associated Timelines	4/17/72
S&E-AERO-106	Pertinent State Vectors Determined in Real-Time by GSFC and MSC and Associated Terminal Conditions	4/20/72
S&E-AERO-107	Postflight Tracking Data, C-Band and USB Measured Parameters	4/19/72
S&E-AERO-109	Postflight S-IVB Telemetered G idance Velocity and Vehicle Attitude Data and Associated Timelines from Translunar Injection to Loss of Telemetry	4/28/72
S&E-AERO-110	S-IVB Spent Stage Predicted Disposal Trajectory	4/1/72
S&E-AERO-111	S-IVB Spent Stage Preflight Targeting Objectives	2/14/72

SECTION 1

INTRODUCTION AND SUMMARY

The AS-511 flight (Apollo 14 mission) was launched at 17:54:00 GMT on April 16, 1972. S-IVB stage reignition occurred during the first TLI opportunity and the second burn of the S-IVB stage injected the spacecraft onto a translunar trajectory. Following translunar injection, the Command and Service Module (CSM) was separated and docked with the Lunar Module (LM) and the combination was ejected from the S-IVB/IU stage. A series of maneuvers of the S-IVB/IU spent stage followed resulting in a lunar impact trajectory. This report discusses the reconstruction of the different maneuvers experienced by the spent stage, the analysis of tracking data from the Spaceflight Tracking and Data Network, the resulting best-estimate trajectory, and the associated lunar impact point.

The AS-511 S-IVB/IU lunar impact mission objectives are:

a. The lunar impact point should be within 350 km of the preselected target at 2.3 degrees south latitude and 31.7 degrees west longitude.

b. The actual impact point should be determined within 5 km (0.165 degree).

c. The time of impact should be determined within 1 second.

The loss of signal and the associated tracking data on April 17, 1972, at 21:03:59 GMT precluded determining the impact location and time within the 5-km and 1-second mission objectives. The impact location and time reported by the principal seismic investigator, Dr. Gary Latham, and calculated from lunar impact seismic data is not reported to within the latter two mission objectives.

The final determination of the impact point is

2.24 ± 0.33 degrees north latitude and
24.49 ± 0.33 degrees west longitude

on April 19, 1972 at 21:02:02. This location, determined by trajectory reconstruction, is 258 km northeast of the target and is within the 350-km mission objective. This impact point is within 8 km of the impact location calculated from the recorded seismic data. The lunar impact point, reconstructed from the tracking data, is considered accurate in position to within 10 km. The time quoted above is taken from the lunar seismic data calculation and is considered accurate to within 2 seconds. The lunar impact point and associated data presented in this report supersedes the data presented in Reference 1.

SECTION 1 (Continued)

During the Apollo 16 mission, the Lunar Impact Team changed the targeting activities considerably from preflight planned operations because of the following real-time indications:

a. IU GN_2 cooling pressurant leakage.

B. Unanticipated IU velocity accumulations prior tc Timebase 8.

c. Suspected early S-IVB APS Module 1 propellant depletion.

d. Unsymmetrical APS ullage performance.

Because of these indications, a more efficient LOX dump attitude was selected to reduce the APS targeting burn requirement. Due to the problems with the vehicle, there would have been no opportunity to perform a second APS burn even if it had been required.

Following passive thermal control (PTC) initiation, a significant increase in the angular momentum of the vehicle occurred during the early portion of the PTC time period. This angular momentum increase is attributed to reactions of the S-IVB/IU stage to some combination of several small forces present on the stage. Also, small translational accelerations of the stage observed in the tracking data during the early PTC time period are attributed to these small forces.

The lunar impact conditions, together with several items of significance derived from the analysis and the best-estimate trajectory, are described in Section 2. The data used in the analysis and the accuracy of the best-estimate trajectory are discussed in Section 3. All times quoted in this report are Greenwich Mean Time (GMT). The ephemeris used for the analysis is JPL DE19 with a time correction of 42.35 seconds. Latitude and longitude in this report are quoted as positive north and east, respectively, unless otherwise noted.

Appendix A describes the methods used to analyze the tracking data and the Instrument Unit's velocity measurements. Appendix B presents a time history of trajectory parameters from CSM/LV separation to lunar impact.

SECTION 2

BEST-ESTIMATE TRAJECTORY AND LUNAR IMPACT MANEUVERS DISCUSSION

The AS-511 S-IVB/IU trajectory presented in this report represents the best estimate of the actual trajectory. A list of significant events associated with this trajectory is presented in Table 2-I. Loss of the downlink signal at 21:03:59, April 17, 1972, limited data coverage after CSM/LV separation to the first 24 hours of a possible 72-hour tracking period. Appendix B contains a listing of significant parameters of the trajectory at selected time points from CSM/LV separation to lunar impact.

The following three periods of flight were established for the purpose of reconstructing the best-estimate trajectory listed in Appendix B.

a. Pre-PTC Time Arc - from CSM/LV separation to PTC initiation (23:49:06, April 16, 1972).

b. Early PTC Time Arc - from 00:00:00 until 04:00:00, April 17, 1972.

c. Late PTC Time Arc - from 04:00:00 until 21:03:59, April 17, 1972.

Tracking data during these three time arcs were used with the Lunar Impact Determination (LID) program to determine associated best-estimate trajectory segments. Appendix A contains a brief description of the LID program.

This section discusses the following four areas of significant interest with the trajectory information derived from the three trajectory segments associated with the time arcs listed above:

a. CSM/LM Docking, Ejection, and Evasive Maneuvers.

b. Safing (CVS Venting and LOX Dump) and Lunar Impact Targeting Maneuvers.

c. Passive Thermal Control and Perturbations.

d. Lunar Impact Conditions.

Although the prime objective of this report is to present the findings associated with Item (d) above, this analysis is extended to provide a reconstruction of the various maneuvers noted in Items (a) through (c) above.

SECTION 2 (Continued)

Figure 2-1 presents line-of-sight range-rate residuals from Goldstone (GDSW) and Hawaii (HAW3) tracking stations. These residuals graphically depict the major S-IVB/IU velocity changes arising from the different maneuvers. Residuals are obtained by differencing observed range and range-rate data from a tracking station with calculated range and range-rate data from a sophisticated orbital model fitting portions of the data (observed minus calculated). For Figure 2-1, an orbital model containing reconstructed maneuvers is fitted to observed pre-PTC tracking data taken between 21:12:00 and 23:48:00, April 16, 1972. Figure 2-1 residuals are then generated by propagating the reconstructed CSM/LV separation state vector forward without using any model of the maneuvers.

Telemetered IU accelerometer data after CSM/LV separation are used to assist in reconstructing the various maneuvers depicted in Figure 2-1 which are used in the pre-PTC data fit. Figure 2-2 indicates the validity of the reconstructed maneuvers by showing Goldstone (GDSW), Merritt Island (MIL3), and Hawaii (HAW3) line-of-sight range-rate residuals obtained from the LID program which propagated forward the reconstructed CSM/LV separation state vector and used the modeled maneuvers. The maneuvers are modeled such that during the entire pre-PTC period the residuals of the tracking data are less than ±0.05 m/s, the quantization level of the accelerometer data. Table 2-II summarizes the significant reconstructed maneuvers experienced by the S-IVB/IU following CSM/LV separation. The calculated directions of the accelerations caused by the maneuvers are also presented in Table 2-II for comparison with the platform gimbal angles.

Figure 2-3 shows the accumulated AS-511 Instrument Unit platform velocity data during the time period from CSM/LV separation through the APS lunar impact burn. Figure 2-4 provides the platform gimbal angles during the same time period.

2.1 CSM/LM DOCKING, EJECTION, AND EVASIVE MANEUVERS

CSM/LV separation occurred at 20:58:59, April 16, 1972, and docking occurred 1,014 seconds later at 21:15:53. CSM/LM ejection occurred at 21:53:15 with the APS evasive burn attitude maneuver initiated 646 seconds later at 22:04:01. The 80-second APS evasive burn was initiated at 22:12:08, one second later than Timebase 8 initiation.

Although the docking maneuver is visible in the tracking residuals of Figure 2-2, the velocity change due to docking is insignificant on the scale of quantization of the accelerometer data. Therefore, there is no docking maneuver entry in Table 2-II.

2.1 (Continued)

The reconstructions of the ejection and evasive burn maneuvers are depicted in Table 2-II. The reconstructed ejection pitch and yaw angles differ by 3 and 5 degrees, respectively, from the platform gimbal angles. Since the velocity change is not too large, these differences are not significant. The reconstructed evasive burn yaw angle compares well with the platform yaw gimbal angle. However, the evasive burn pitch angles differ by 10 degrees confirming an unsymmetrical APS ullage performance.

2.2 SAFING AND LUNAR IMPACT TARGETING MANEUVERS

Following the APS evasive burn, a LOX dump attitude maneuver was initiated at 22:21:48 (see Figure 2-4). Because of the unsymmetrical APS performance and a suspected early depletion of the APS Module 1 propellant, the Lunar Impact Team at the Huntsville Operations Support Center decided in real time to place the S-IVB/IU in a more efficient LOX dump attitude than preflight planned. This attitude change was to reduce later APS burn requirements. A 300-second CVS vent was initiated at 22:28:47, April 16, 1972, and 280 seconds later the 48-second LOX dump was initiated at 22:33:27.

After these two safing maneuvers were completed, an APS burn attitude maneuver was started at 23:24:37. A 54-second APS lunar impact burn was then initiated at 23:34:07, April 16, 1972. Because of problems with the vehicle, listed in Section 1, no other APS burn was attempted (see Reference 1).

The reconstruction of the above three maneuvers is depicted in Table 2-II. The reconstructed pitch and yaw angles for the CVS vent differ from the platform gimbal angles by 6 and 8 degrees, respectively. This may indicate the CVS velocity change is not along the longitudinal axis of the vehicle but, since the accelerometer changes are quite small, these differences may not be significant. The reconstructed LOX dump pitch and yaw angles compare favorably with the platform gimbal angles (see Table 2-II). Again, the differences shown in Table 2-II between the reconstructed APS impact burn angles and the platform gimbal angles of 7 and 3 degrees in pitch and yaw, respectively, confirm an unsymmetrical APS ullage performance.

2.3 PASSIVE THERMAL CONTROL AND PERTURBATIONS

Following the APS lunar impact burn, S-IVB/IU stage roll, pitch, and yaw body rates of +0.5 degree/second, -0.3 degree/second, and -0.3 degree/second, respectively, were commanded at 23:49:06, April 16, 1972, to initiate a three-axis tumbling

2.3 (Continued)

motion. Approximately 17 seconds later, at 23:49:23, the flight control computer was commanded off leaving the S-IVB/IU stage with a rotational motion about the C.G. This rotational motion provided passive thermal control (PTC). Also, the three-axis tumbling motion was planned to minimize the translational effect of any post-APS S-IVB/IU stage related perturbing forces by distributing their effects in all directions about the coasting stage's C.G. motion.

Figure 2-2, depicting GDSW, MIL3, and HAW3 line-of-sight range-rate residuals, shows the initiation of the PTC maneuver and that the tumbling motion is superimposed upon the C.G. translational motion. This range rate modulation occurs because the stage's rotational antenna motion is not modeled in the LID program; only the C.G. translational motion is modeled. The reconstructed PTC maneuver, presented in Table 2-II, was solved for with the LID program by fitting the early portion of the PTC tracking data and finding the needed velocity change to make the pre-PTC and early PTC residuals compatible.

Figure 2-5 shows Goldstone (GDSW) range-rate tracking residuals during the early portion of the PTC data coverage period. Figure 2-6 shows Tidbinbilla (HSKW) range-rate residuals during the middle portion of the PTC data coverage. Figure 2-7 shows Madrid (MADW) range-rate residuals during the latter portion of the PTC data coverage. A significant increase in the frequency of the tumble modulation of the range rate (5.4 cph to 10.4 cph) can be observed in the GDSW and HSKW residuals (see Figures 2-5 and 2-6) during the period from about 00:00:00 to 11:00:00, April 17, 1972. Thereafter, the MADW residuals (see Figure 2-7) show a gradual frequency decrease (10.3 cph to 9.0 cph) from about 12:00:00 to 21:00:00, April 17, 1972 (also, see Figure 3-5).

An analysis of the early PTC residuals, using a model of the motion of a rigid rod about the C.G., simulating the rotating S-IVB/IU stage, shows a significant increase of the angular momentum of the vehicle. This momentum increase evidences the presence of small perturbing forces torquing the vehicle (see discussion below). Also, an analysis of the tracking data to reconstruct the C.G. motion gives evidence of small perturbing forces translating the vehicle slightly during the early PTC period (see the discussion in Paragraph 3.2.3).

The S-IVB/IU PTC rotational motion during the lunar impact trajectory was analyzed assuming that the vehicle was a moment-free body and symmetrical about its longitudinal axis. With these assumptions, Euler's moment equations, which describe the rotational motion of the body about its

2.3 (Continued)

C.G., can be solved analytically. The resulting motion can best be visualized by reference to Figure 2-8. As there are no torques on the body, angular momentum is conserved, i.e., the angular momentum vector has constant magnitude and direction in inertial space. The angular momentum vector ($\vec{h}$), the angular velocity vector ($\vec{\omega}$), and the vehicle longitudinal axis (X_B) lie in a plane. This plane rotates (precesses) about the angular momentum vector with angular velocity $\dot{\psi}$. At the same time the body rotates about its longitudinal axis with velocity $\dot{\phi}$. The precession rate, $\dot{\psi}$, the spin rate, $\dot{\phi}$, and the angle between them, θ, are constant with time. The resultant angular velocity, ω, is the vector sum of $\dot{\psi}$ and $\dot{\phi}$ and is constant in magnitude.

The range-rate residuals produced by rotation about the C.G. of the two transponder antennas located on the IU were calculated by first determining the antenna velocities from the cross product of ω with the antenna position vectors relative to the C.G. and then projecting these velocities onto the range vector from the tracker to the vehicle. In order to determine which antenna was being tracked at any given time, an antenna switching criterion was required. For this purpose, it was assumed that the antenna closer to the tracker was the one being tracked. The tracked antenna was determined by projecting the antenna position vectors onto the range vector and noting which projection was smaller in an algebraic sense. The range vector from the tracker to vehicle was obtained as a function of time from the LID program.

This simulation was coupled with a Kalman filter routine to estimate the initial vehicle attitudes and attitude rates which would yield a best fit of the modeled residuals to the observed residuals obtained from the LID program. An initial estimate of the vehicle attitude was obtained from telemetered platform gimbal angles. An estimate of the attitude rates was made by numerically differentiating the gimbal angle time history. Figure 2-9 shows the results obtained with the simulation fitting 42 minutes of GDSW residuals starting at 00:01:00, April 17, 1972. The RMS of the residual differences for this fit is 5.5 mm/s. Discontinuities in the model and actual residuals are the result of antenna switching as the antennas alternately rotate into view of the tracker. Fits over subsequent time spans were obtained for GDSW residuals from 01:01:00 to 01:23:00 and 01:25:00 to 01:42:00, April 17, 1972. A fit of the beginning of the HSKW residuals was also obtained from 06:02:00 to 06:05:00, April 17, 1972.

2.3 (Continued)

The decreasing time spans over which satisfactory fits could be obtained with the moment-free simulation are caused by the previously mentioned increase in frequency of the tumble. Results of these fits are summarized in Table 2-III. The data demonstrates that a significant increase in angular momentum occurred during the time from 00:00:00 to 06:05:00, April 17, 1972, causing the increasing residual frequency observed in Figures 2-5 and 2-6. The data also shows the close correlation of the tumble frequency and $\dot{\psi}$, the precession rate of the vehicle. Analysis of the rate of increase of the angular momentum components during the time from 00:00:00 to 01:24:00, April 17, 1972, shows that an average torque of -0.020 N-M was acting about the vehicle roll axis and a torque of 0.037 N-M was acting about an axis lying in the yaw-pitch plane. The roll moment would require a force of 0.0061 N if applied at the S-IVB circumference. The combined yaw-pitch moment would require a 0.0083 N force if applied near one of the APS modules. The S-IVB contractor, McDonnell-Douglas, reports that small forces exist on the stage of these magnitudes, or an order of magnitude larger, which in some combination could account for these moments. It is to be noted, also, that the last data entry in Table 2-III indicates additional forces began to act following 02:00:00 and before 06:00:00, April 17, 1972, in order to cause the additional increase in angular momentum.

2.4 LUNAR IMPACT CONDITIONS

The AS-511 S-IVB/IU impacted the lunar surface on April 19, 1972, at 21:02:02 ± 2 seconds. The impact coordinates derived from the best-estimate trajectory are:

2.24 ± 0.33 degrees north latitude and
24.49 ± 0.33 degrees west longitude.

The impact point is 258 km northeast of the targeted point, 163 km north of the Apollo 12 seismometer, 278 km northwest of the Apollo 14 seismometer, and 1,118 km southwest of the Apollo 15 seismometer. The final impact point is plotted in Figure 2-10 along with other points of interest. Table 2-IV presents a description of the stage and trajectory parameters at impact. Figure 2-11 defines the incoming heading angle and the impact angle.

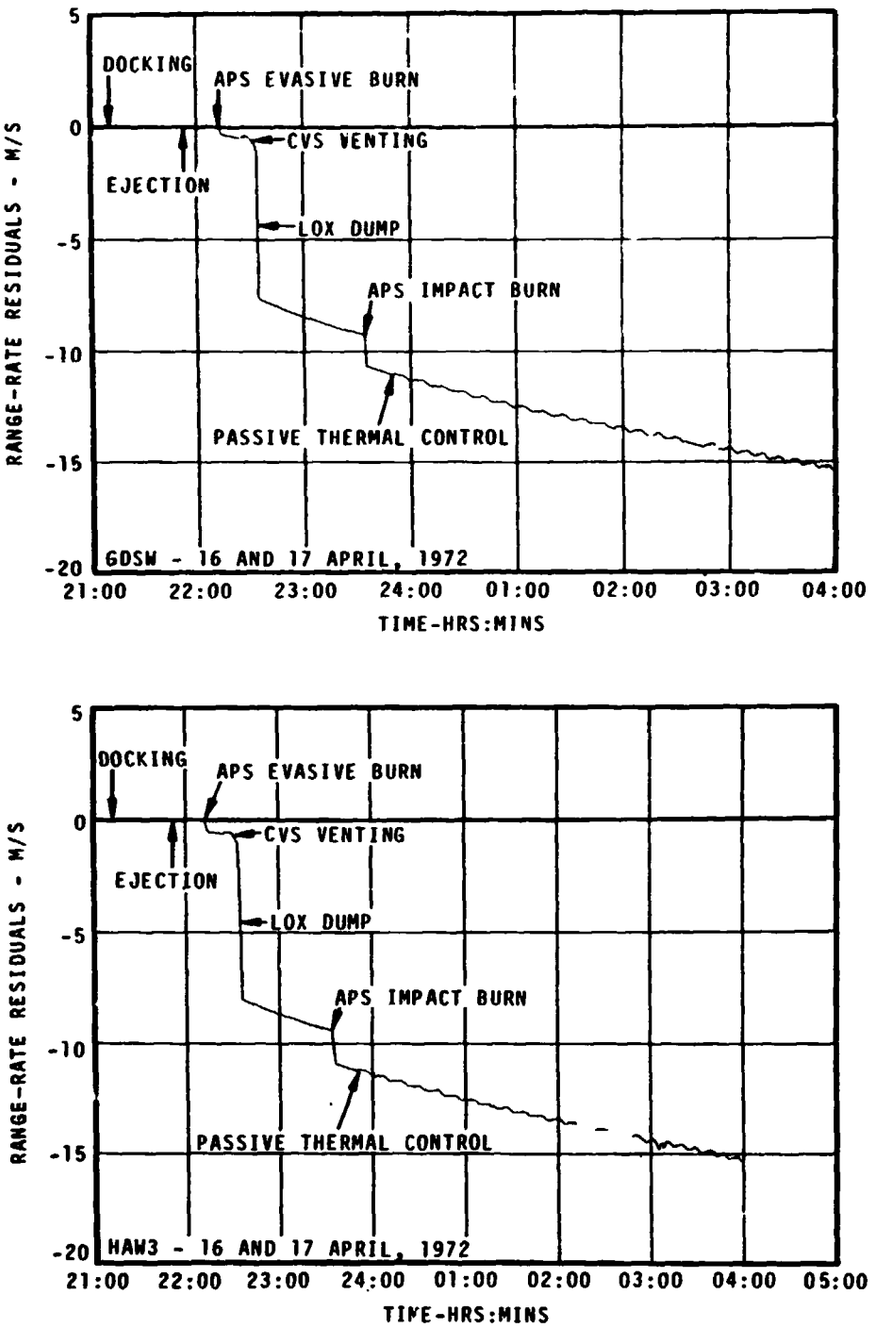

FIGURE 2-1. TRANSLUNAR COAST MANEUVERS OVERVIEW

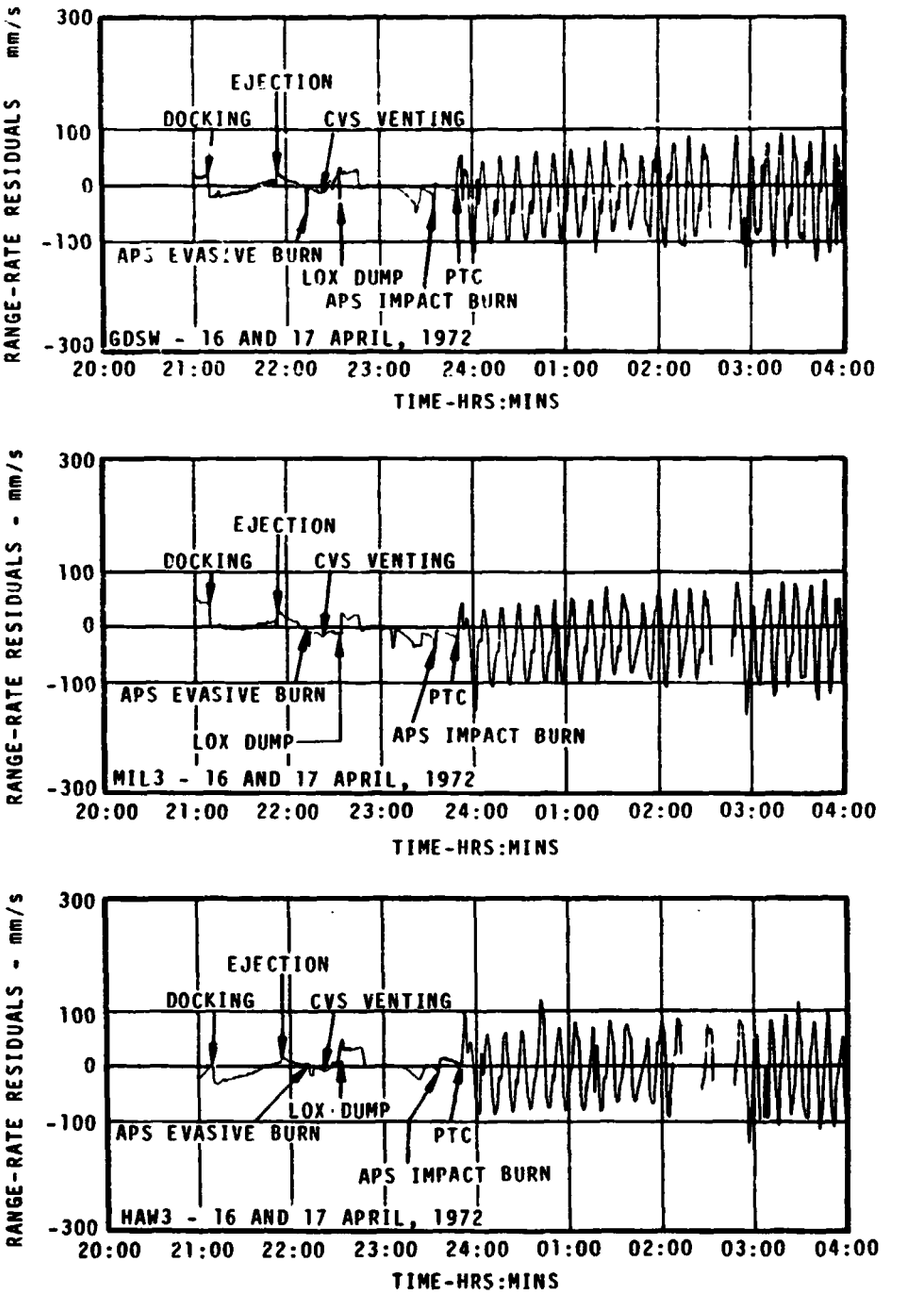

FIGURE 2-2. GOLDSTONE, MERRITT ISLAND, AND HAWAII RANGE-RATE RESIDUALS FOR MODELED TRANSLUNAR COAST MANEUVERS AND EARLY PTC DATA FIT

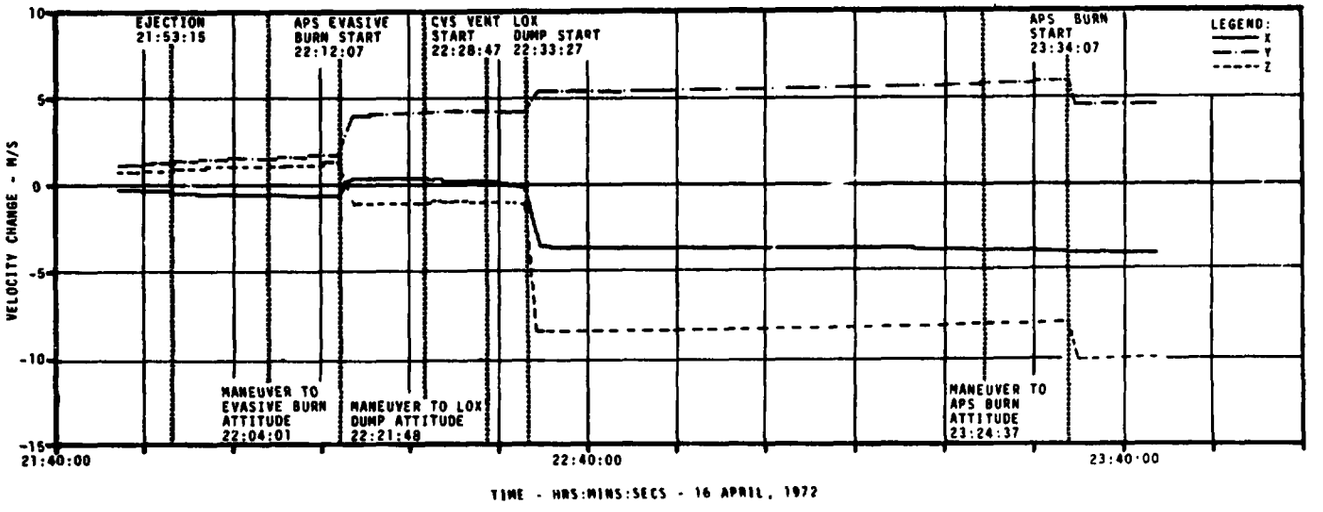

FIGURE 2-3. AS-511 INSTRUMENT UNIT PLATFORM VELOCITY ACCUMULATION DURING LUNAR IMPACT TARGETING

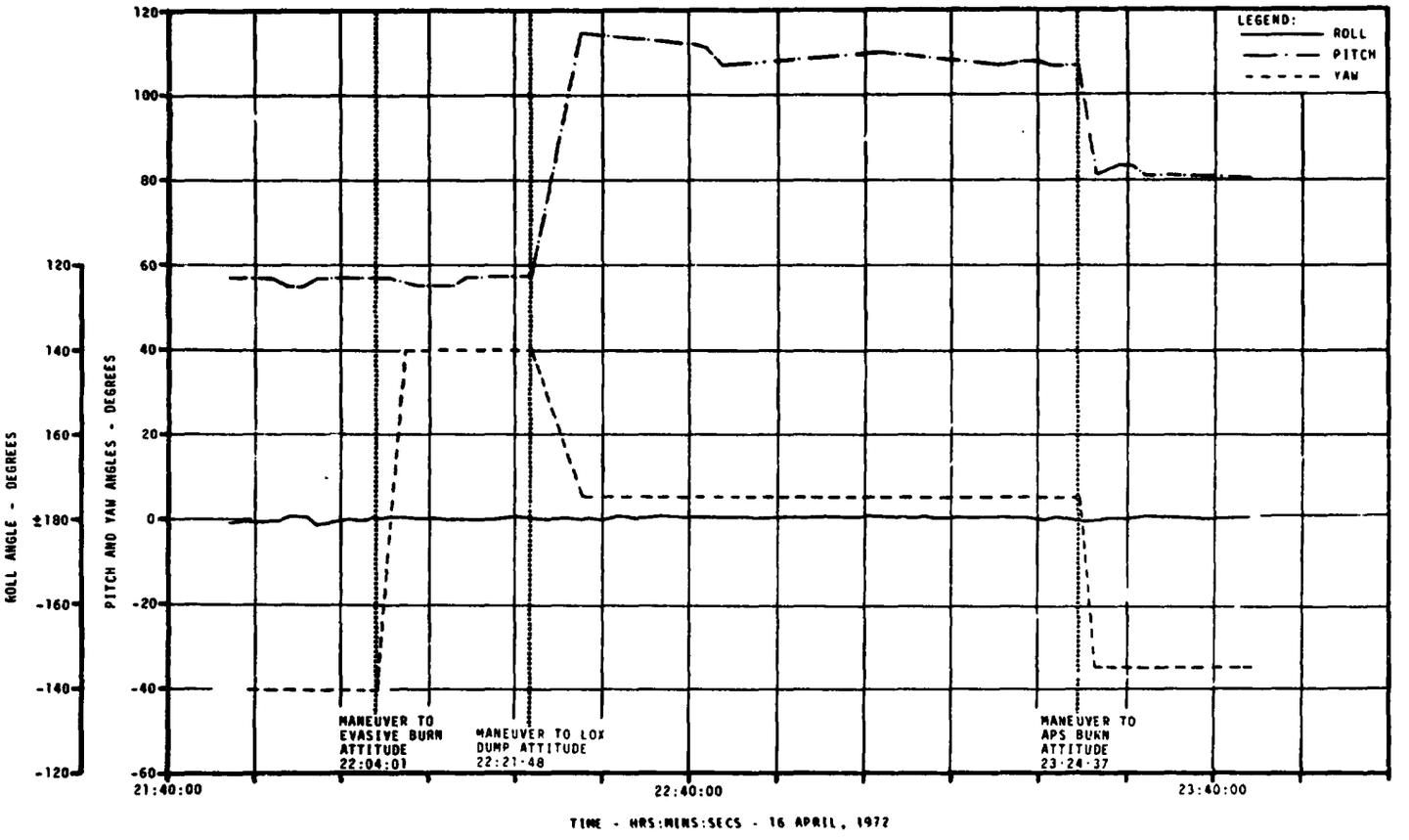

FIGURE 2-4. AS-511 INSTRUMENT UNIT PLATFORM GIMBAL ANGLES DURING LUNAR IMPACT TARGETING

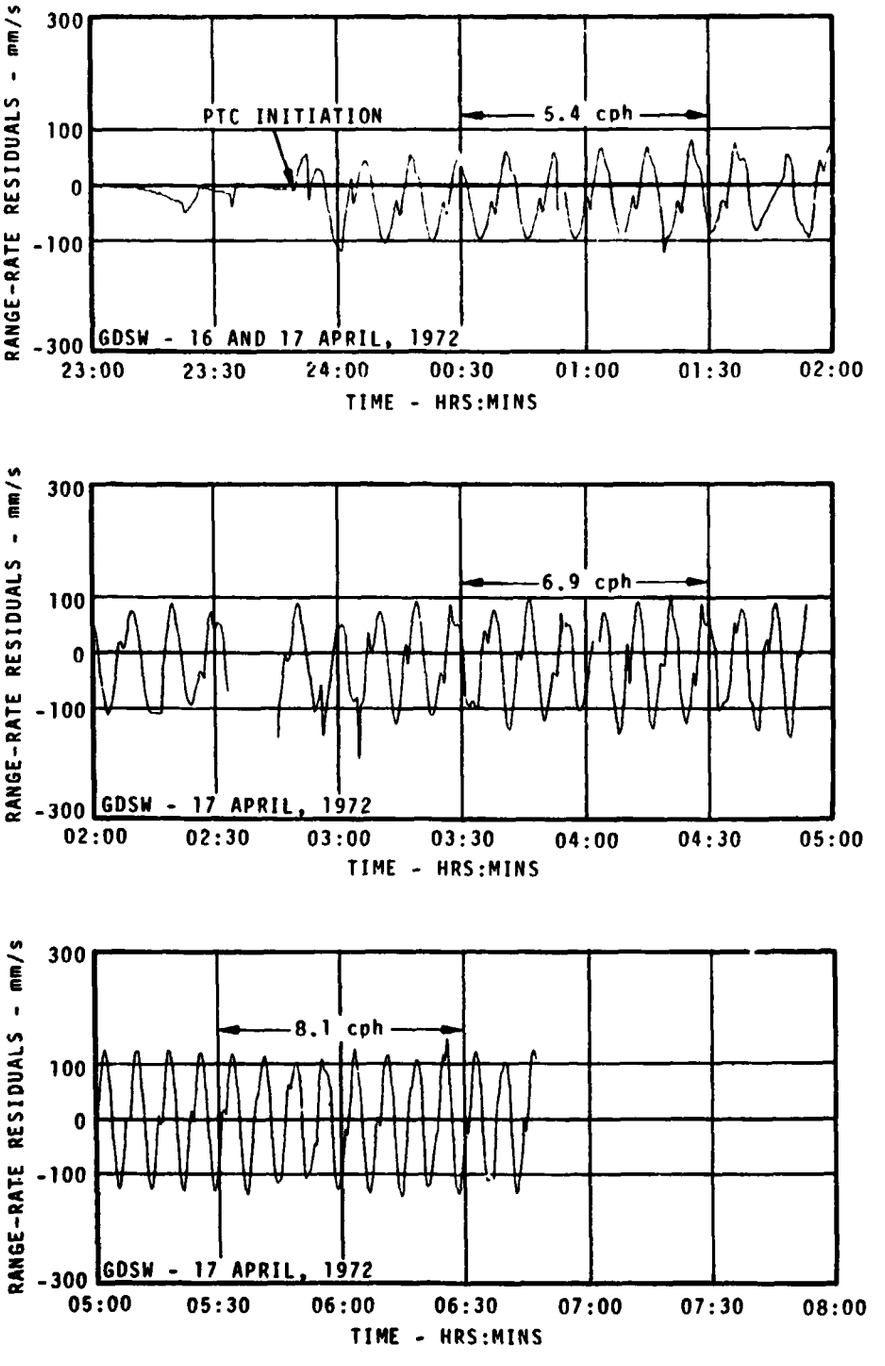

FIGURE 2-5. GOLDSTONE RANGE-RATE RESIDUALS FOR FIRST PART OF PTC DATA ARC

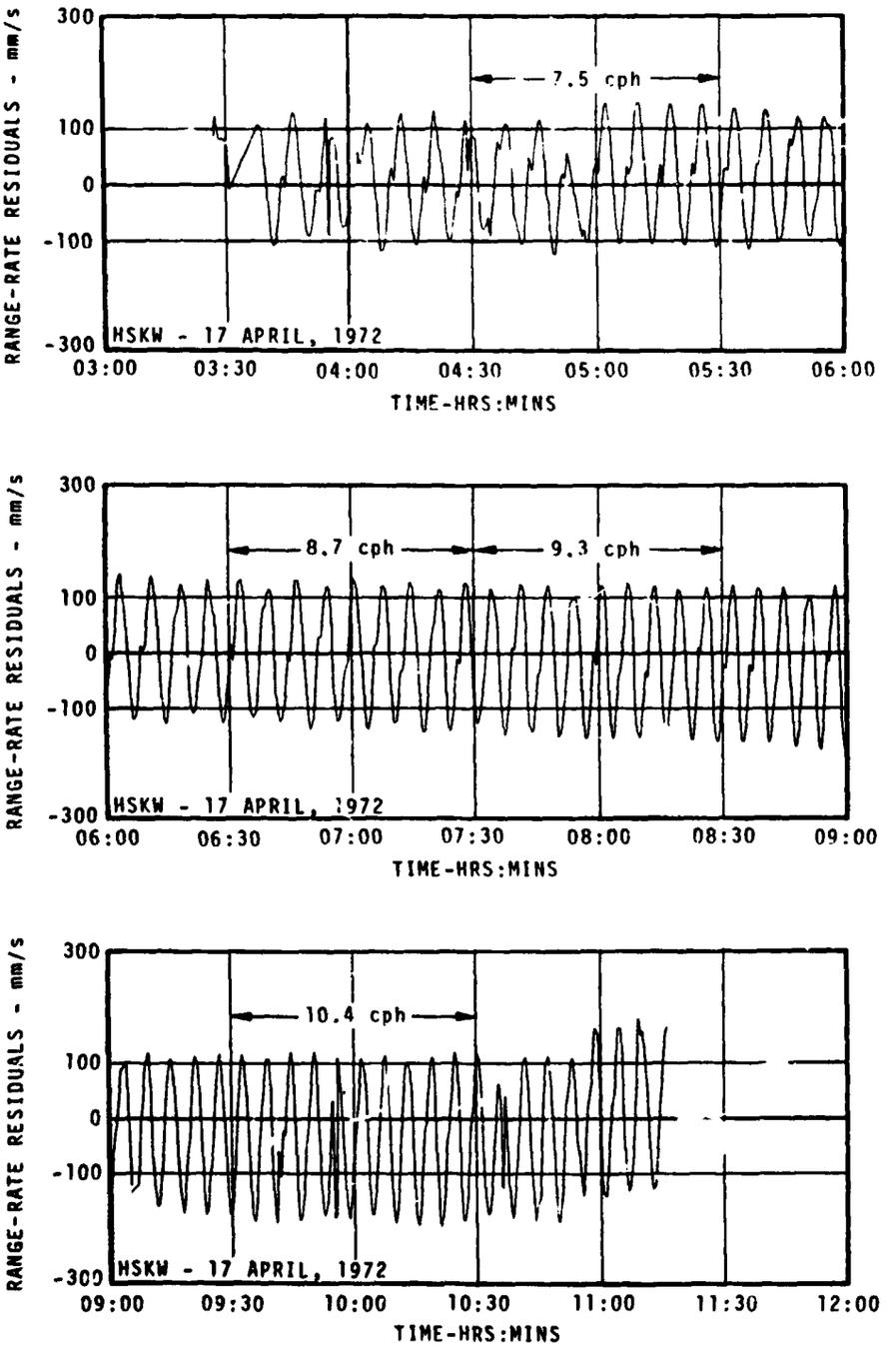

FIGURE 2-6. TIDBINBILLA RANGE-RATE RESIDUALS FOR MIDDLE PART OF PTC DATA ARC

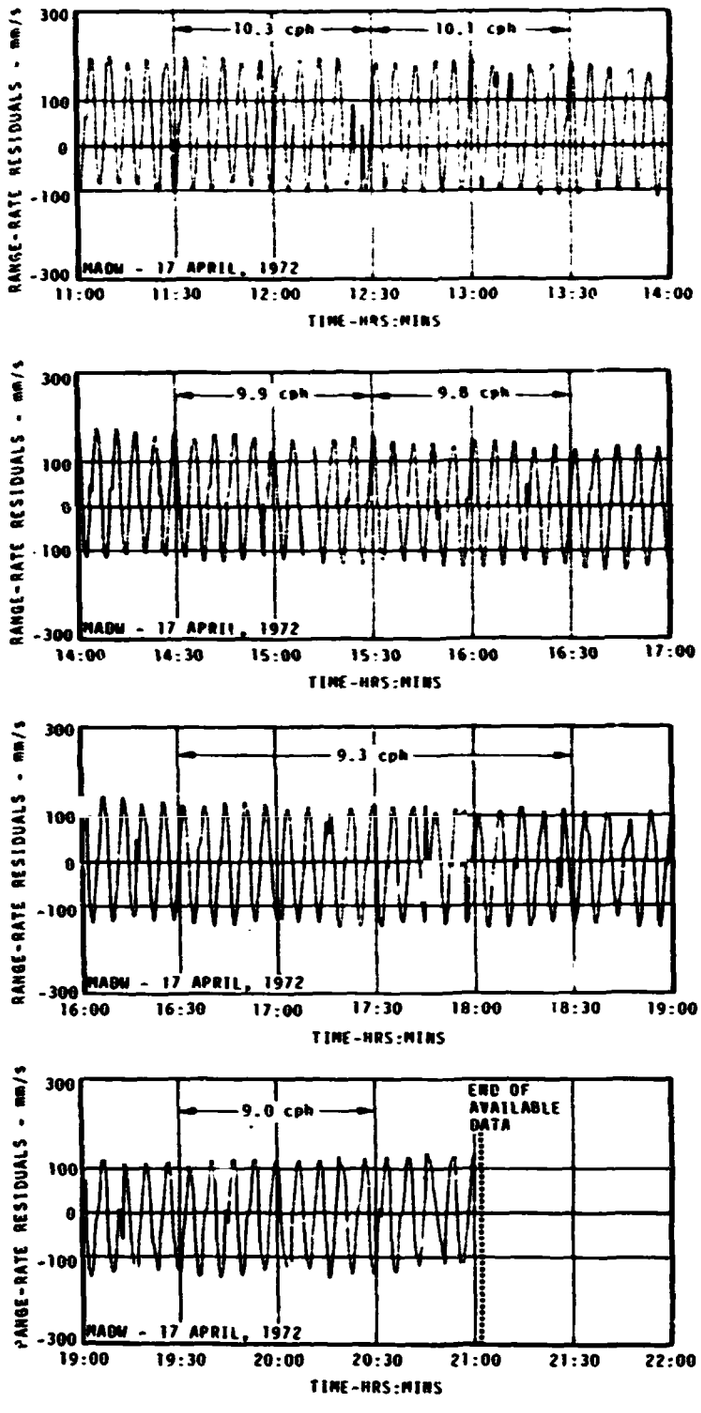

FIGURE 2-7. MADRID RANGE-RATE RESIDUALS FOR LATE PART OF PTC DATA ARC

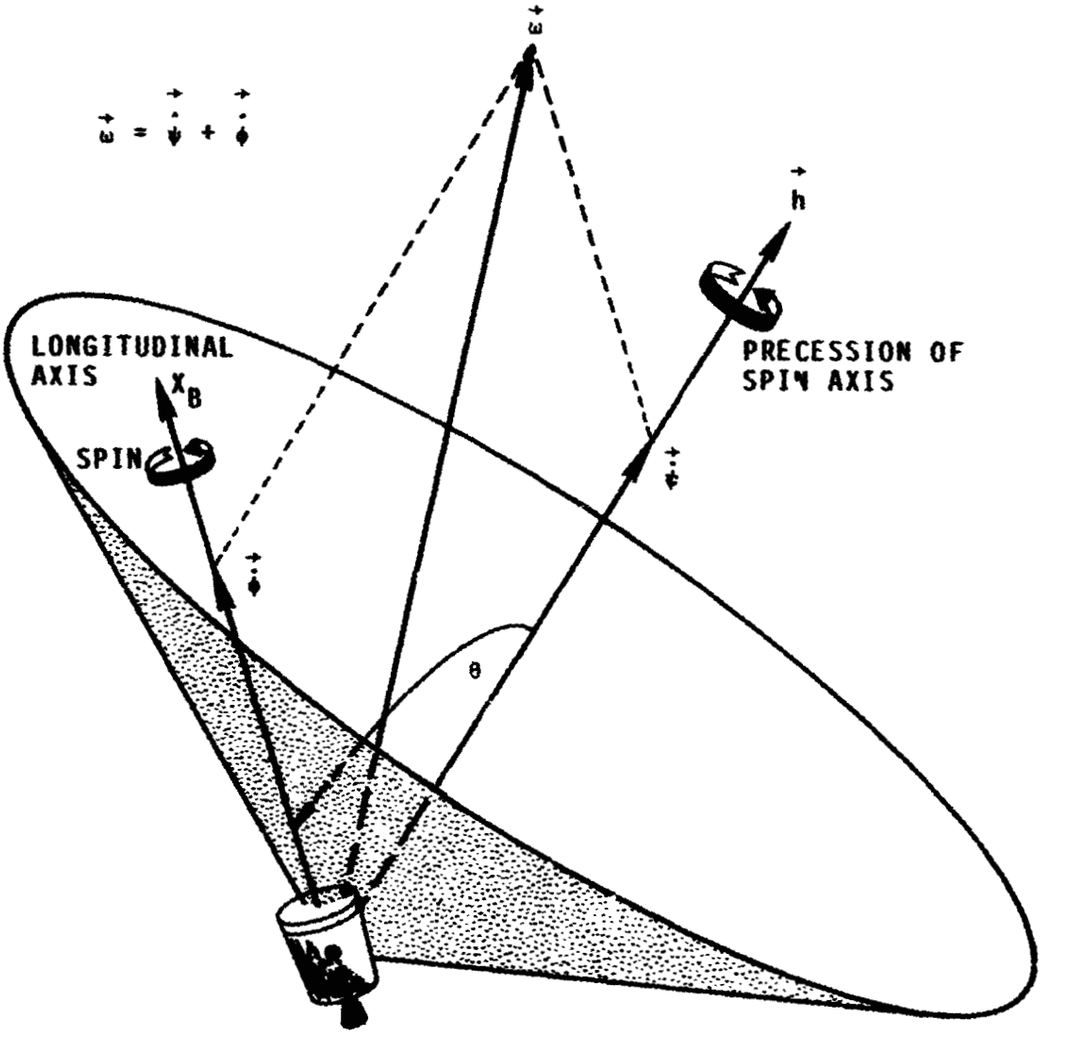

FIGURE 2-8. MOTION OF MOMENT-FREE VEHICLE

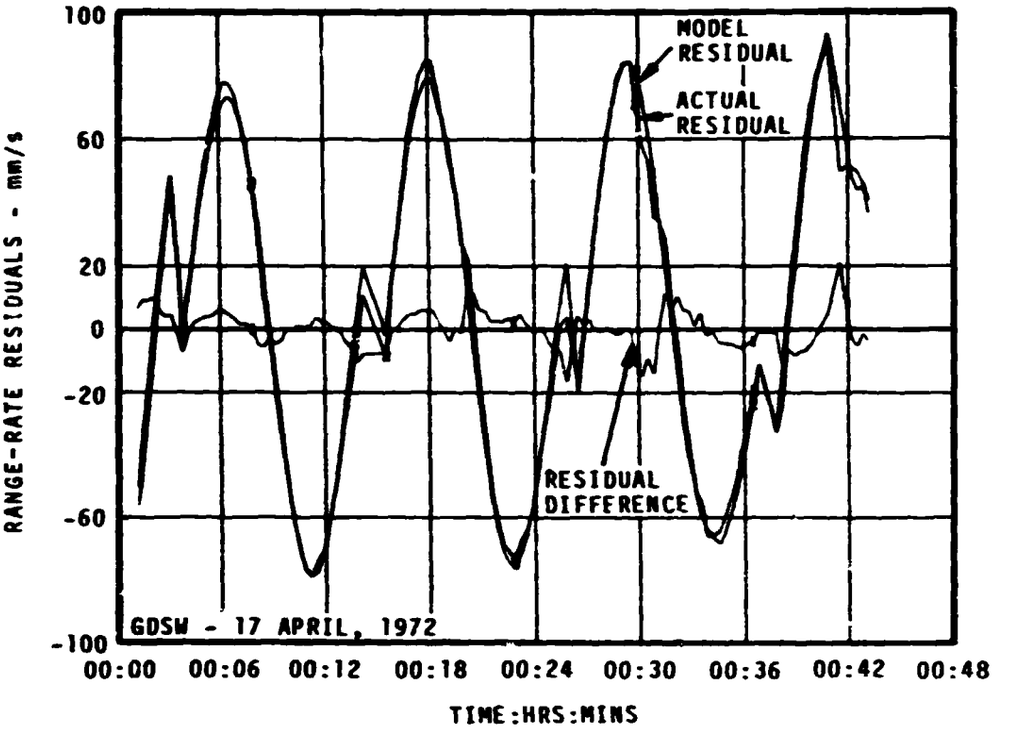

FIGURE 2-9. PTC TUMBLING RECONSTRUCTION

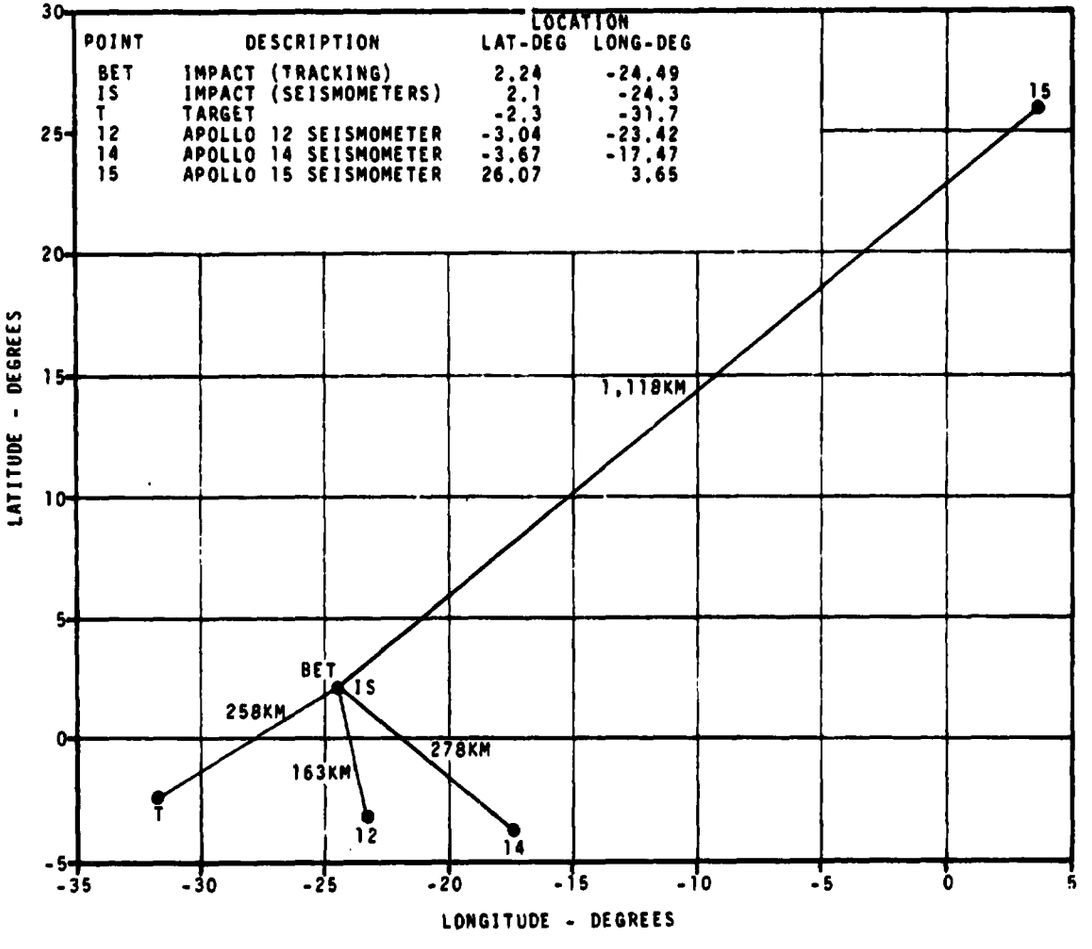

FIGURE 2-10. APOLLO 16 LUNAR LANDMARKS

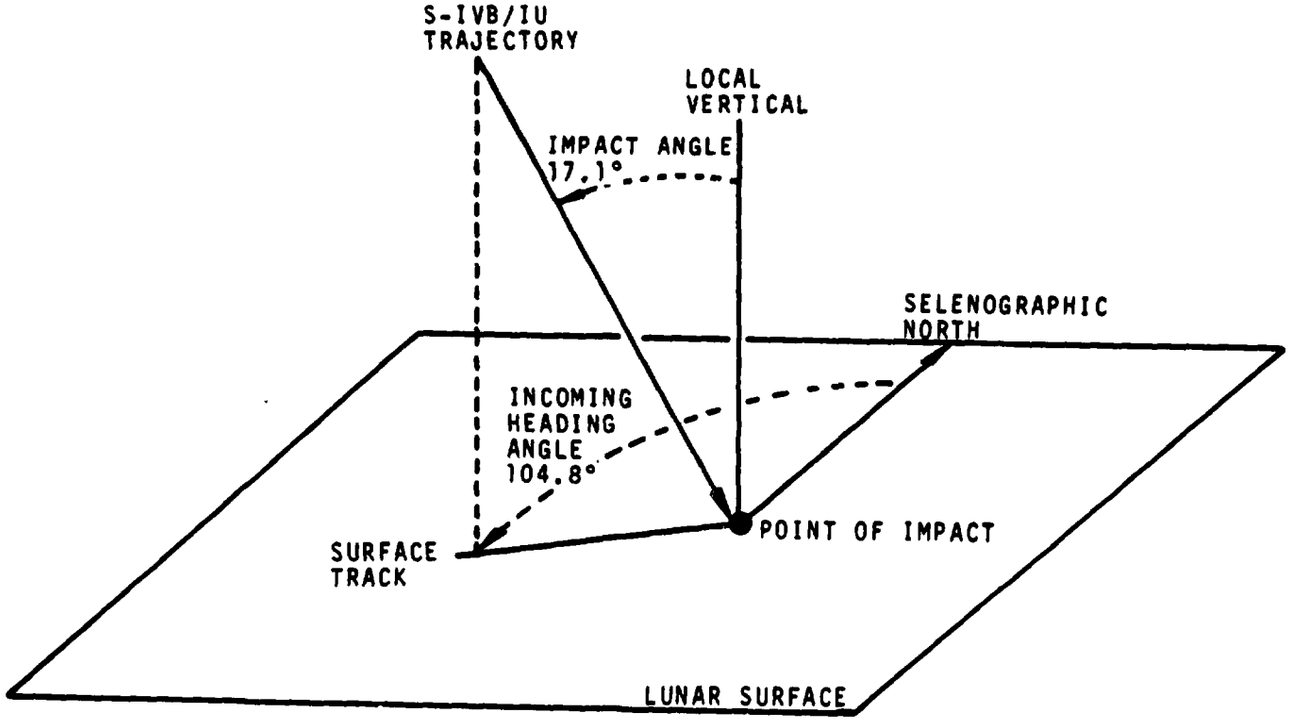

FIGURE 2-11. AS-511 S-IVB/IU LUNAR IMPACT HEADING AND IMPACT ANGLES

TABLE 2-I. SIGNIFICANT EVENT TIMES

EVENT	GREENWICH MEAN TIME HR:MIN:SEC	RANGE TIME HR:MIN:SEC
Range Zero	16 April 1972 17:54:00	00:00:00
CSM/LV Separated	20:58:59	03:04:59
CSM/LM Docked	21:15:53	03:21:53
CSM/LM Ejected	21:53:15	03:59:15
Evasive Burn Attitude Maneuver Initiated	22:04:01	04:10:01
Timebase 8 Initiated	22:12:07	04:18:07
APS Evasive Burn Initiated	22:12:08	04:18:08
LOX Dump Attitude Maneuver Initiated	22:21:48	04:27:48
CVS Vent Initiated	22:28:47	04:34:47
LOX Dump Initiated	22:33:27	04:39:27
APS Impact Burn Attitude Maneuver Initiated	23:24:37	05:30:37
APS Impact Burn Initiated	23:34:07	05:40:07
PTC Commanded	23:49:06	05:55:06
IU Flight Control Computer Inhibit Commanded	23:49:23	05:55:23
CCS Downlink Signal Lost	17 April 1972 21:03:59	27:09:59
Lunar Impact	19 April 1972 21:02:02	75:08:02

TABLE 2-II. RECONSTRUCTED LUNAR IMPACT MANEUVERS

PARAMETER	CSM/LM EJECTION	APS EVASIVE BURN	CVS VENT	LOX DUMP	APS IMPACT BURN	PTC INITIATION
Initiation 16 April Hr:Min:Sec	21:53:15	22:12:08	22:28:47	22:33:27	23:34:07	23:49:06
Duration, sec	25*	80	280	48	54	170
PACSS13 Acceleration						
$\ddot{X}$, mm/s^2	-6.000	12.250	-0.893	-71.458	0.000	0.527
$\ddot{Y}$, mm/s^2	7.200	27.500	0.393	20.417	-24.074	-0.345
$\ddot{Z}$, mm/s^2	8.000	-29.375	-1.571	-150.830	-40.370	0.087
Velocity Change, M/S	-0.308	3.365	0.518	8.071	2.538	0.108
effective pitch, deg	53	67	120	115	90	9
effective yaw, deg	-36	41	13	7	-31	-33
Vehicle Gimbal Angles						
pitch, deg	56	57	114	114	83	NA
yaw, deg	-41	41	5	6	-34	NA

*Arbitrary duration

NOTE: The IU platform (and PACSS13) were aligned as follows: X-axis vertical up from Pad 39A (28.608422° latitude and -80.604133° longitude) at 17:53:43.037 on 16 April, 1972; Z-axis downrange along a 72.0344° launch azimuth; Y-axis completes the right hand system.

TABLE 2-III. PTC TUMBLING ANALYSIS RESULTS

DATA ARC 17 APRIL HR:MIN	h N-M-SEC	θ DEG	$\dot{\phi}$ DEG/SEC	ω DEG/SEC	$\dot{\psi}$ DEG/SEC	CPH	TUMBLE FREQUENCY* CPH
00:01 to 00:43	5,092	81.52	0.308	0.631	0.507	5.07	5.2
01:01 to 01:23	5,206	82.67	0.272	0.618	0.522	5.22	5.4
01:25 to 01:42	5,251	82.36	0.286	0.629	0.523	5.23	5.4
06:02 to 06:05	7,938	85.84	0.236	0.843	0.792	7.92	8.1

*Frequencies as observed in the LID residuals (see Figures 2-5 and 2-6)

Note: See Figure 2-8 for a diagram of the motion of a moment-free vehicle.

TABLE 2-IV. STAGE AND TRAJECTORY IMPACT PARAMETERS

PARAMETER	VALUE
Dry Stage Mass, kg	∿13,973
Velocity Relative to Surface, km/s	2.561
Kinetic Energy, joules x 10^9	∿46
Impact Angle Measured from Vertical, deg	17.1
Incoming Heading Angle Measured from North to West, deg	104.8
Mean Lunar Radius, km	1,738.09
Selenographic Longitude, deg	-24.49
Selenographic Latitude, deg	2.24
Impact Time, Hr:Min:Sec, on 19 April 1972	21:02:02
Distance to Target, km	258
Distance to Apollo 12 Seismometer, km	163
Distance to Apollo 14 Seismometer, km	278
Distance to Apollo 15 Seismometer, km	1,118

THIS PAGE LEFT BLANK INTENTIONALLY

SECTION 3

BEST-ESTIMATE TRAJECTORY DETERMINATION

The best-estimate trajectory determined in this analysis consists of three separate trajectory segments corresponding to the three time arcs outlined in Section 2. Tracking data available during these three arcs were used to determine initial state vectors with components consisting of appropriate combinations of initial positions, velocities, and where needed, acceleration biases over selected time periods. The initial position and velocity values were then propagated forward by integrating the LID program model equations with the solved-for acceleration biases. The trajectory listing presented in Appendix B was derived from these three separate trajectory segments.

This section discusses the data used in the analysis, the reconstruction of the three trajectory segments, the associated data residuals, and the estimated accuracy of the different segments. This section also establishes the basis for the quoted uncertainty in the impact point.

3.1 DATA UTILIZATION

The tracking data used for this analysis came from eleven USB and two C-band radar stations as listed in Table 3-I. The station locations listed in this table are taken from Reference 2. The time spans of the data used in this analysis are shown in bar chart form in Figure 3-1 for both range rate and range data. Different portions of the data were used to establish the separate trajectory segments as discussed below.

3.1.1 Pre-PTC Time Arc Data Utilization

The best estimate of the pre-PTC segment was established from 391 range-rate measurements from five USB tracking stations and 312 range measurements from two C-band tracking stations. The breakdown by station and the time arcs of data used for each are presented in Table 3-II.

3.1.2 Early PTC Time Arc Data Utilization

The best estimate of the early PTC segment was established from 356 range-rate measurements from three USB stations (Goldstone - 125 points, Merritt Island - 128 points, and Hawaii - 103 points), 29 range measurements from two USB stations (Goldstone - 11 points, Merritt Island - 18 points), and 10 range measurements from the Bermuda C-band tracking station. The time arc of the data used spans the interval from

3.1.2 (Continued)

23:54:00, April 16, to 04:00:00, April 17, 1972 (see Figure 3-1). This data was used primarily to reconstruct the PTC maneuver as noted in Paragraph 2.3.

3.1.3 Late PTC Time Arc Data Utilization

The best estimate of the late PTC segment was established from 2,558 selected range-rate measurements from eight USB tracking stations and 163 range measurements from three USB tracking stations. The breakdown by station and the time arcs of data used for each are presented in Table 3-III. As noted in Section 2, the loss of the downlink signal at 21:03:59, April 17, 1972, limits the tracking data for this segment to the first 21 hours of a possible 69-hour tracking interval.

3.2 TRAJECTORY ANALYSIS AND ACCURACY

Each of the trajectory segments composing the best-estimate trajectory was established separately by using the data discussed above.

The quality of a particular trajectory solution can be judged by examining the tracking data residuals. Large residual means or skewness indicate failure to fit the data. These tracking data residuals are obtained by differencing the observed data from a tracking site with calculated data from a tracking model based upon a particular trajectory segment. All tracking data residuals presented in this report consist of differences between observed and calculated quantities (O-C).

3.2.1 Pre-PTC Trajectory Segment Analysis and Accuracy

The tracking data outlined in Paragraph 3.1.1, over a time period of 2 hours and 36 minutes which included the modeled maneuvers, were used in the LID program to obtain the pre-PTC trajectory segment. A solution was obtained for an initial vector at CSM/LV separation. This vector, propagated forward with the applicable maneuvers listed in Table 2-II, produces the appropriate data points in Appendix B and the residual plots shown in Figure 2-2. As noted in Section 2, the initial state propagated forward without the maneuvers produces the residuals depicted in Figure 2-1.

Figure 3-2 depicts the range-rate residuals from the Bermuda (BDA3) and Greenbelt (ETC3) USB tracking stations during the pre-PTC time arc. Figure 2-2 shows the residuals for the Goldstone (GDSW), Merritt Island (MIL3), and Hawaii (HAW3)

3.2.1 (Continued)

USB tracking stations during both the pre-PTC time arc and the early PTC time arc. The pre-PTC residuals in Figure 2-2 are used in judging the accuracy of the pre-PTC trajectory segment. Figure 3-3 shows the range residuals for the Bermuda (BDQC) and Merritt Island (MILC) C-band tracking stations. Note: The range deviations evident in Figure 3-3 after PTC initiation indicate a negligibly small velocity error in modeling the PTC maneuver (see Paragraph 3.2.2). The residual statistics for the pre-PTC data fit are presented in Table 3-II. Based upon the good quality of the fit through the entire maneuver period, the accuracy of the trajectory segment during the pre-PTC time period is estimated to be within ±200 m in radius magnitude and ±100 mm/s in velocity magnitude.

3.2.2 Early PTC Trajectory Segment Analysis and Accuracy

The tracking data outlined in Paragraph 3.1.2 above, over a time period of four hours, were used to obtain the reconstructed PTC maneuver shown in Table 2-II.

The LID program, using initial position and velocity components from the end of the pre-PTC trajectory segment, was used to fit the early PTC data and solve for acceleration biases having a 170-second time period starting at PTC initiation. The reconstructed PTC maneuver was then incorporated into the modeled maneuvers so that Figures 2-2, 2-5, 2-6, 2-7 and 3-3 could be generated and the appropriate trajectory point in Appendix B listed. Figure 2-2 shows that the early PTC range-rate data for the GDSW, MIL3 and HAW3 tracking stations are reasonably fit. Figures 2-5, 2-6, and 2-7, besides showing the tumbling frequency increase and subsequent decrease, also show that no major translational accelerations after PTC initiation occurred in the remaining portion of the flight covered by the tracking data. Figure 3-3 shows the range residuals for BDQC and MILC C-band tracking stations following PTC initiation.

These early PTC range residuals show that the reconstructed PTC maneuver has a small, but negligible, velocity error remaining (of the order of 20 mm/s) after fitting the data and solving for the maneuver as described above. Based upon the reasonable fit of the early PTC data, as shown in Figures 2-5, 2-6, and 3-3, plus early PTC range residual means and sigmas, respectively, of GDSW (10 and 21 meters) and MIL3 (68 and 56 meters) tracking stations, the accuracy of the early PTC trajectory segment is estimated to be within ±200 m in radius magnitude and ±100 mm/s in velocity magnitude.

3.2.3 Late PTC Trajectory Segment Analysis and Accuracy

The tracking data outlined in Paragraph 3.1.3, over a time period of 21 hours, were used in the LID program to obtain the late PTC trajectory segment. Initial attempts to properly fit all or significant portions of the 21 hours of data available after 00:00:00, April 17, 1972, with a gravitational model were marginally acceptable. Range and range-rate residual statistics and trends plus time histories of changes in the initial state for various gravitational model fits were greater than desired except for a combination of data over the last three hours before CCS downlink signal loss (see Run A2 in Table 3-V).

Table 3-IV shows the residual statistics for the best gravitational model fit (see Run A20 in Table 3-V) of the data over a time arc from 04:00:00 to 21:00:00, April 17, 1972. Figure 3-4 shows the range residuals from the three USB tracking stations providing range measurements (Goldstone-GDSW, Tidbinbilla-HSKW, and Madrid-MADW). Though the range residuals and trends are small, they evidence small non-gravitational forces acting during the first part of the late PTC trajectory segment. Since the angular momentum increase during this same time period also evidences small forces acting (see Section 2), small unbalanced translational effects may also be expected. Therefore, in order to improve the data fitting during the first part of the late PTC trajectory segment, small non-gravitational accelerations were added to the gravitational acceleration model.

The LID program was used to solve for a number of initial position and velocity components plus small non-gravitational acceleration biases over various time periods by using different combinations of range and range rate data over different time arcs and different stations. Table 3-V gives the impact conditions derived from a set of solutions which have acceptable residual statistics and trends. The final period for the non-gravitational forces was selected to correspond to the period of tumble frequency increase. Figure 3-5 presents a plot of the tumble frequency correlated with the trajectory solutions listed in Table 3-V.

Table 3-III gives a statistical summary of the run selected as the best-estimate trajectory. These residual statistics should be contrasted with the best gravitational fit statistics listed in Table 3-IV. The initial position and velocity state obtained from the best-estimate trajectory were propagated forward with the solved-for non-gravitational biases added to the gravitational model for the appropriate time period to obtain a best-estimate of the lunar impact location and the trajectory points listed in Appendix B.

3.2.3 (Continued)

Figure 3-6 shows three sets of USB range residuals (GDSW, HSKW, MADW) for the best-estimate trajectory and should be contrasted with Figure 3-4 to note the improvement in the fit of the range data sets. The shift (26 km) in the impact point from the best gravitational fit (Run A20) to the point obtained from the best-estimate trajectory should be noted. Figures 3-7, 3-8, and 3-9 show the range-rate residuals for nine USB tracking stations. Based upon the quality of the trajectory fit, the accuracy of the best-estimate trajectory segment during the late PTC data period is estimated to be within ±100 m in radius magnitude and ±50 mm/s in velocity magnitude.

3.3 LUNAR IMPACT POINT ACCURACY

The final lunar impact location is 2.24 degrees north longitude and 24.49 degrees west longitude. The accuracy of the impact coordinates are estimated at ±0.33 degree in both latitude and longitude. Figure 3-10 is a plot of the solutions listed in Table 3-V along with the 3σ circle about the best-estimate solution representing the impact coordinate accuracies. The ±0.33 degree accuracies are based upon the nearly even distribution in latitude and longitude of a large number of lunar impact solutions exemplified by nine solutions listed in Table 3-V which have standard deviations of ±0.29 degree in latitude and ±0.27 degree in longitude. The quoted accuracy above also correlates well with the 3σ ellipse shown in Figure 17 of Reference 2 for the Apollo 16 S-IVB tracking evaluation. In Reference 2, a set of parameters representing initial state errors, station noise values, range-rate biases, station survey uncertainties, and refraction noise were propagated to the moon by an Error Analysis for Satellite to Satellite Tracking (EASST) computer program to give the referenced 3σ ellipse. A check on the ±0.33 degree accuracy (equivalent to 10 km) was also made by propagating the covariance matrix of the best-estimate initial state to the moon, diagonalizing it, and noting that the largest position related eigenvalue is compatible with the quoted accuracy.

Table 3-VI shows lunar impact seismic recorded data. Calculations made using the lunar seismic data gave an impact location of 2.1 degrees north latitude and 24.3 degrees west longitude at 21:02:02, April 17, 1972. The accuracy of the location based upon the seismic calculation is given as an ellipse having a semi-major axis of 20 km, a semi-minor axis of 5 km and the semi-major axis oriented 30 degrees east of north. The accuracy of the time, based upon the seismic calculation, is given as ±2 seconds.

3.3 (Continued)

The time of lunar impact quoted in Sections 1 and 2 is taken from the seismic calculation since the deviation in time obtained from the trajectory reconstruction runs listed in Table 3-V is ±10 seconds. Note: The best-estimate trajectory time of impact, 21:01:55 ±10 seconds, April 19, 1972, spans the seismic calculated impact time. The 7-second difference in the two mean impact times is attributed in part to ephemeris errors (i.e. distance from earth to moon) and uncertainties in the local lunar elevation. It is also to be noted that the best-estimate trajectory impact location is within 8 km of the seismic calculated location.

The above considerations show that the loss of the tracking data precludes the determination of the mission objectives of 5 km and 1 second. However, the location of the impact is within the 350-km mission objective of the target.

DATA TYPE	STATION	NO. OF POINTS
RANGE RATE	MADW	3,007
	GDSW	2,756
	GDS8	1,138
	HSKW	2,623
	ACN3	1,046
	ETC3	1,417
	BDA3	218
	MIL3	2,099
	HAW3	1,390
	GWM3	792
	CRO3	1,519
RANGE	MADW	103
	GDSW	16
	HSKW	49
	MIL3	22
	BDQC	2,610
	MILC	3,799

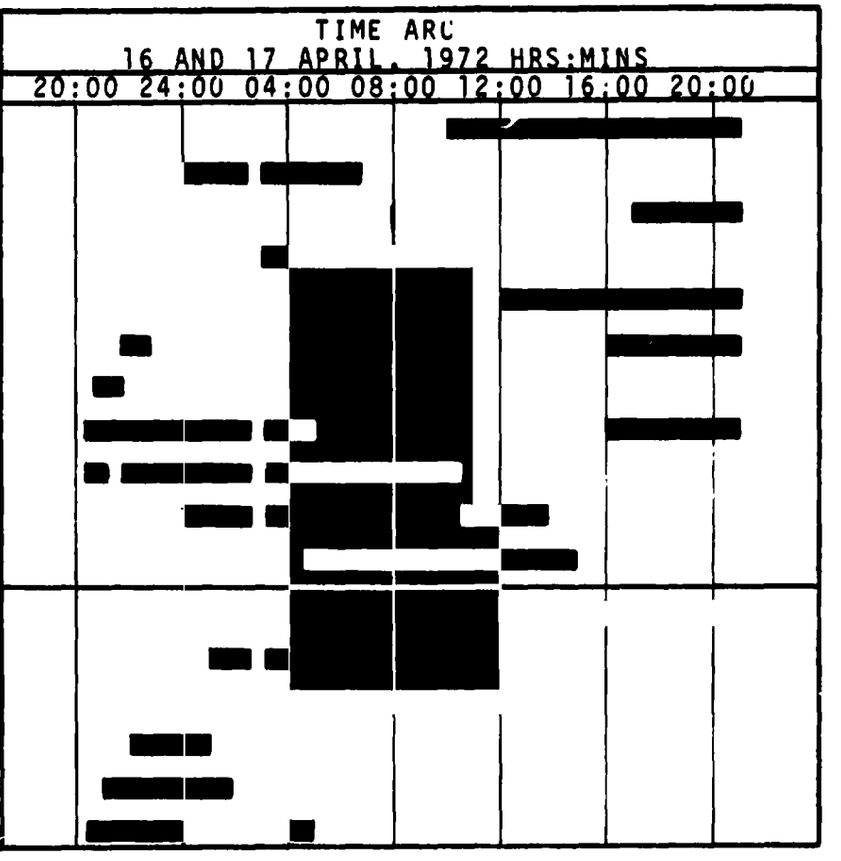

FIGURE 3-1. AS-511 S-IVB/IU TRACKING DATA AVAILABILITY

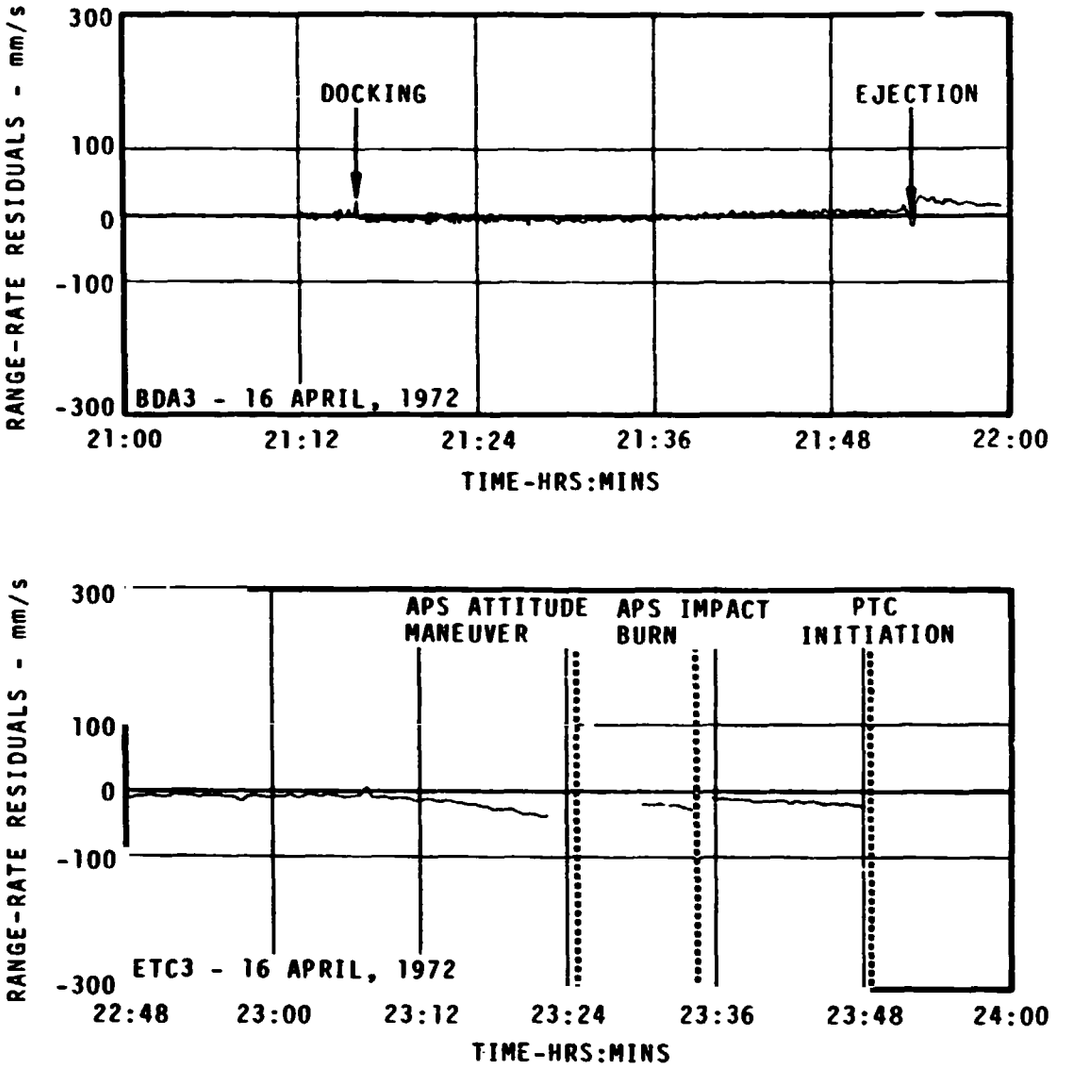

FIGURE 3-2. BERMUDA AND GREENBELT RANGE-RATE RESIDUALS FOR PRE-PTC DATA FIT

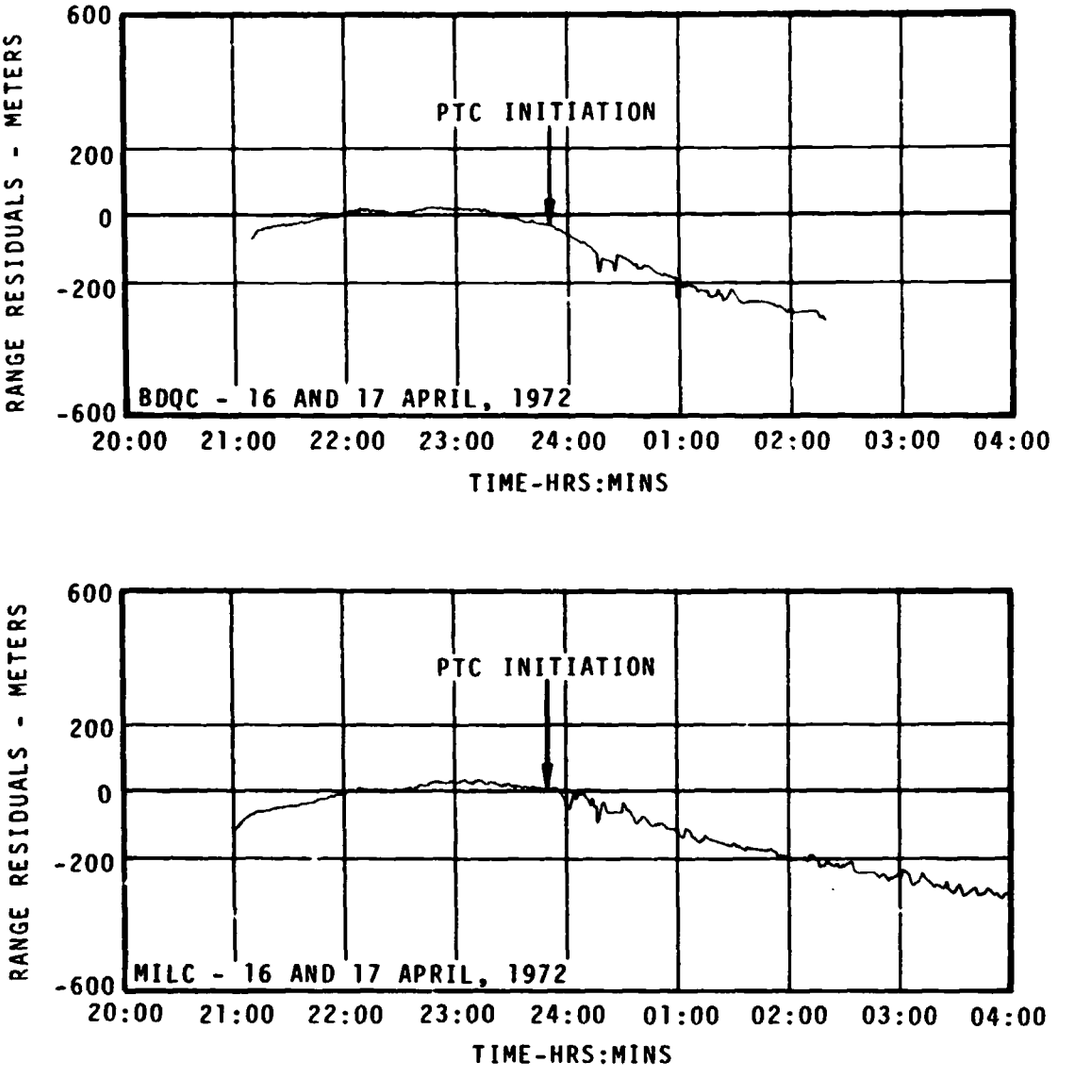

FIGURE 3-3. BERMUDA AND MERRITT ISLAND C-BAND RANGE RESIDUALS FOR PRE-PTC DATA FIT

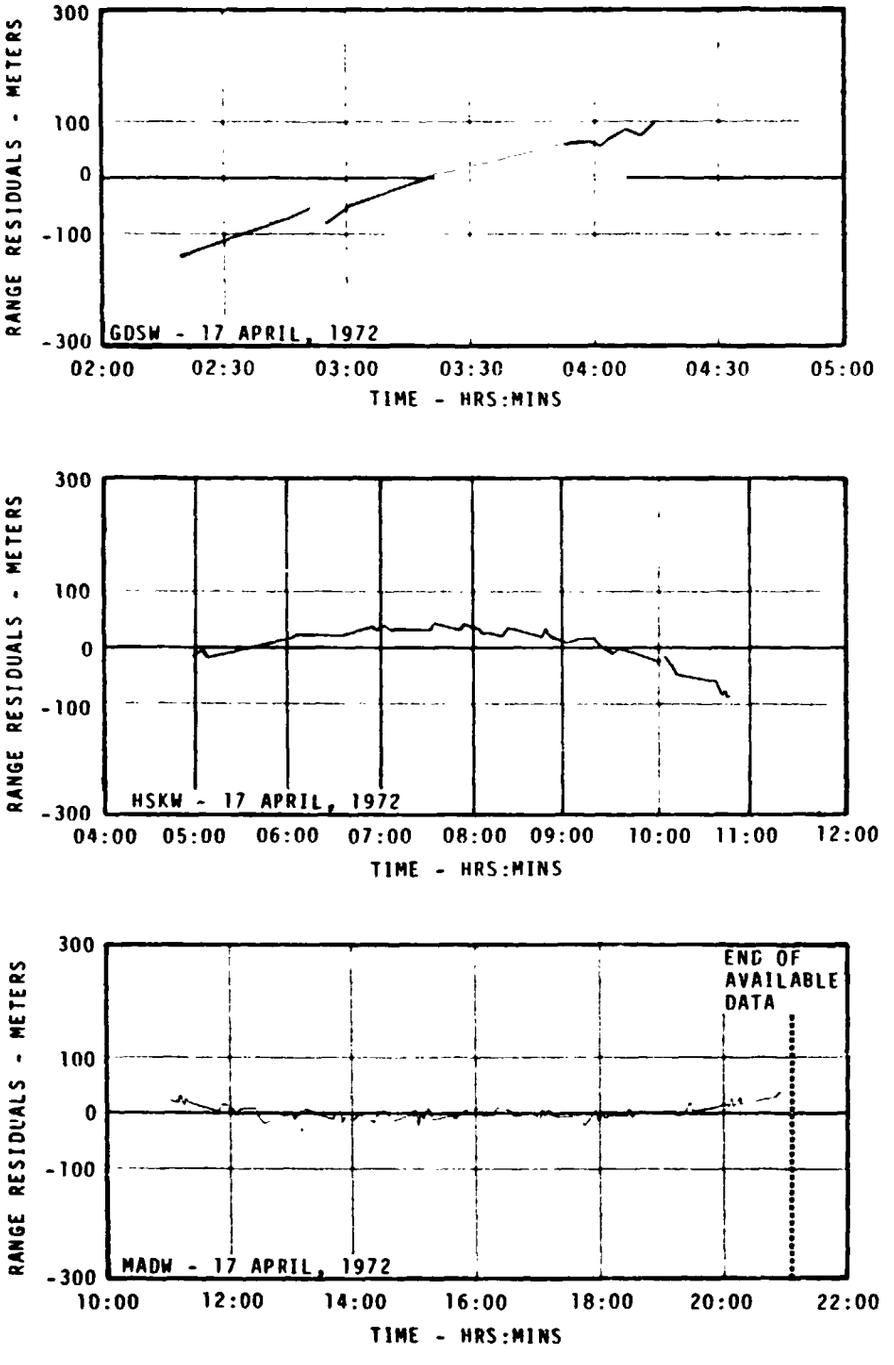

FIGURE 3-4. GOLDSTONE, TIDBINBILLA, AND MADRID USB RANGE RESIDUALS FOR LATE PTC DATA FIT/BEST GRAVITATIONAL MODEL

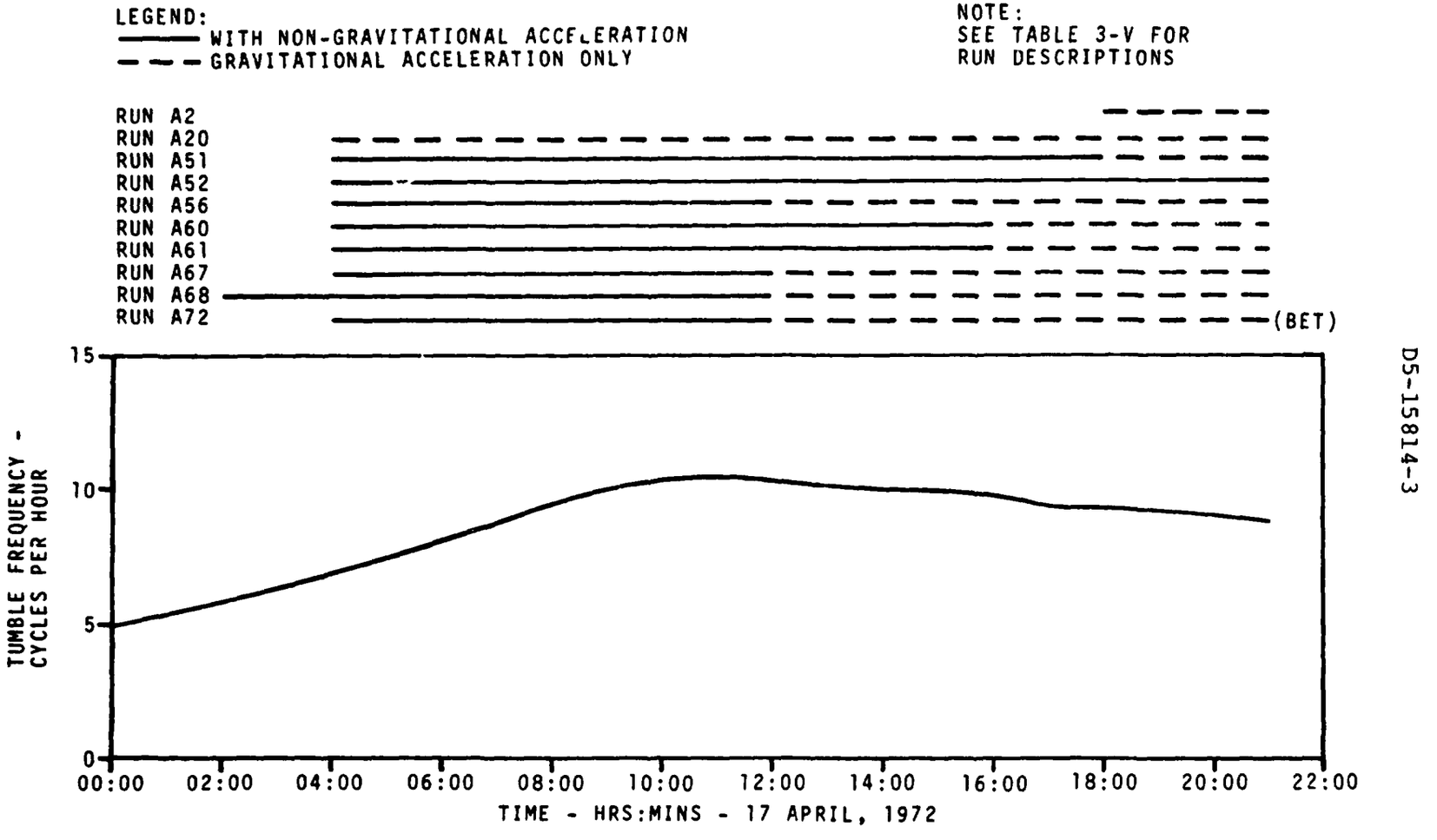

FIGURE 3-5. CORRELATION OF TUMBLE FREQUENCY AND TRAJECTORY SOLUTIONS

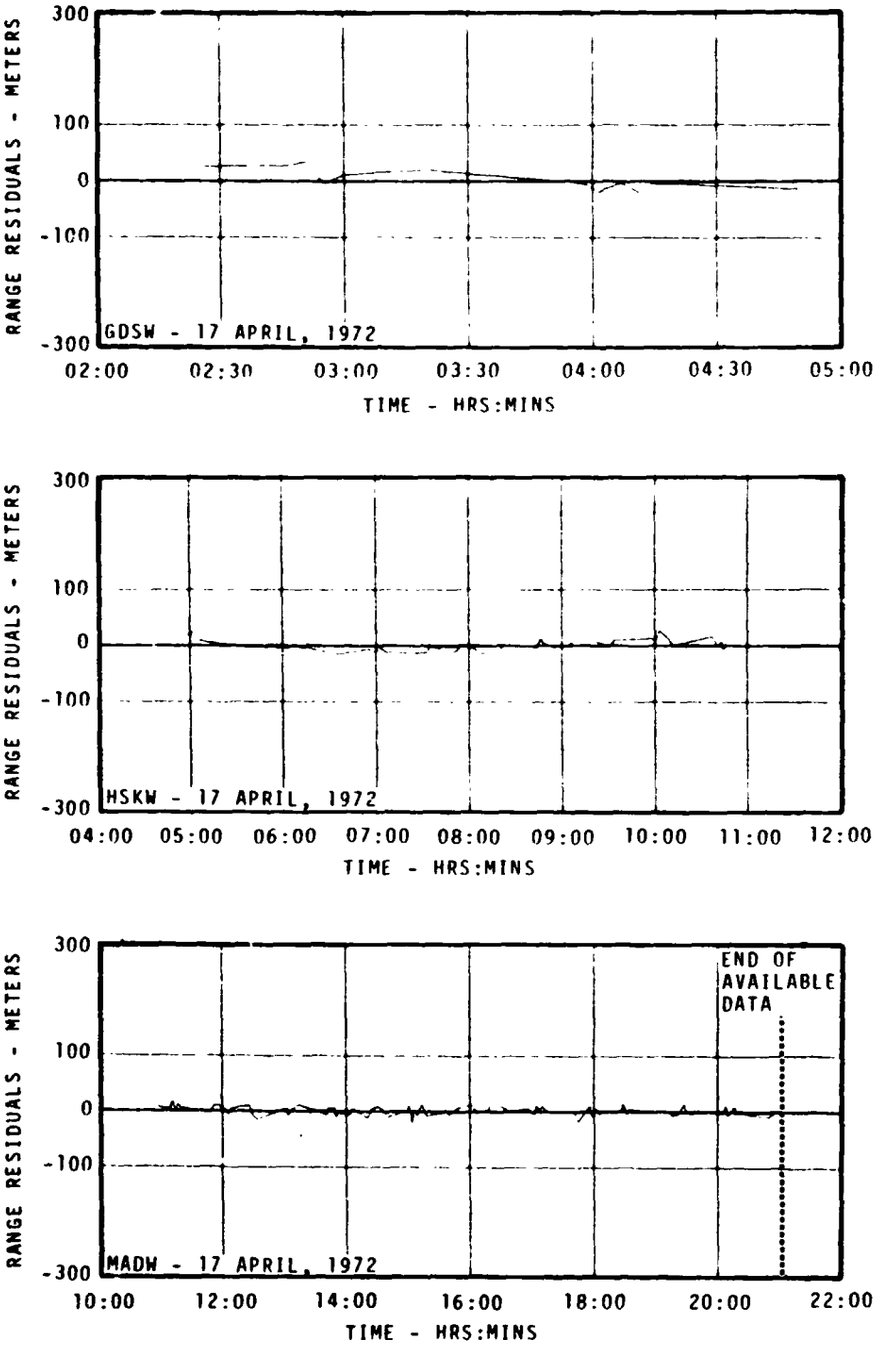

FIGURE 3-6. GOLDSTONE, TIDBINBILLA, AND MADRID USB RANGE RESIDUALS FOR LATE PTC DATA FIT/BEST-ESTIMATE TRAJECTORY

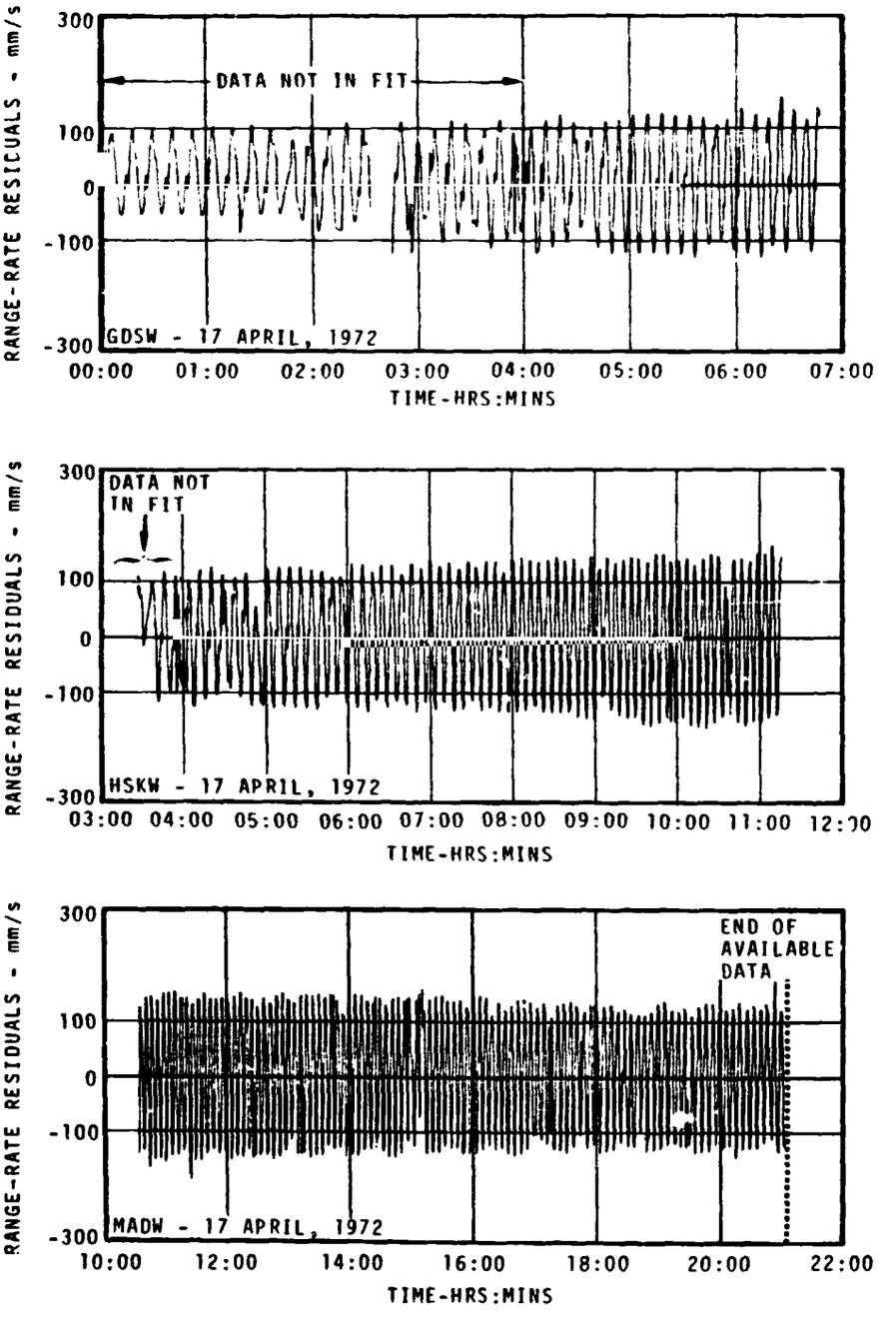

FIGURE 3-7. GOLDSTONE, TIDBINBILLA, AND MADRID RANGE-RATE RESIDUALS FOR LATE PTC DATA FIT/BEST-ESTIMATE TRAJECTORY

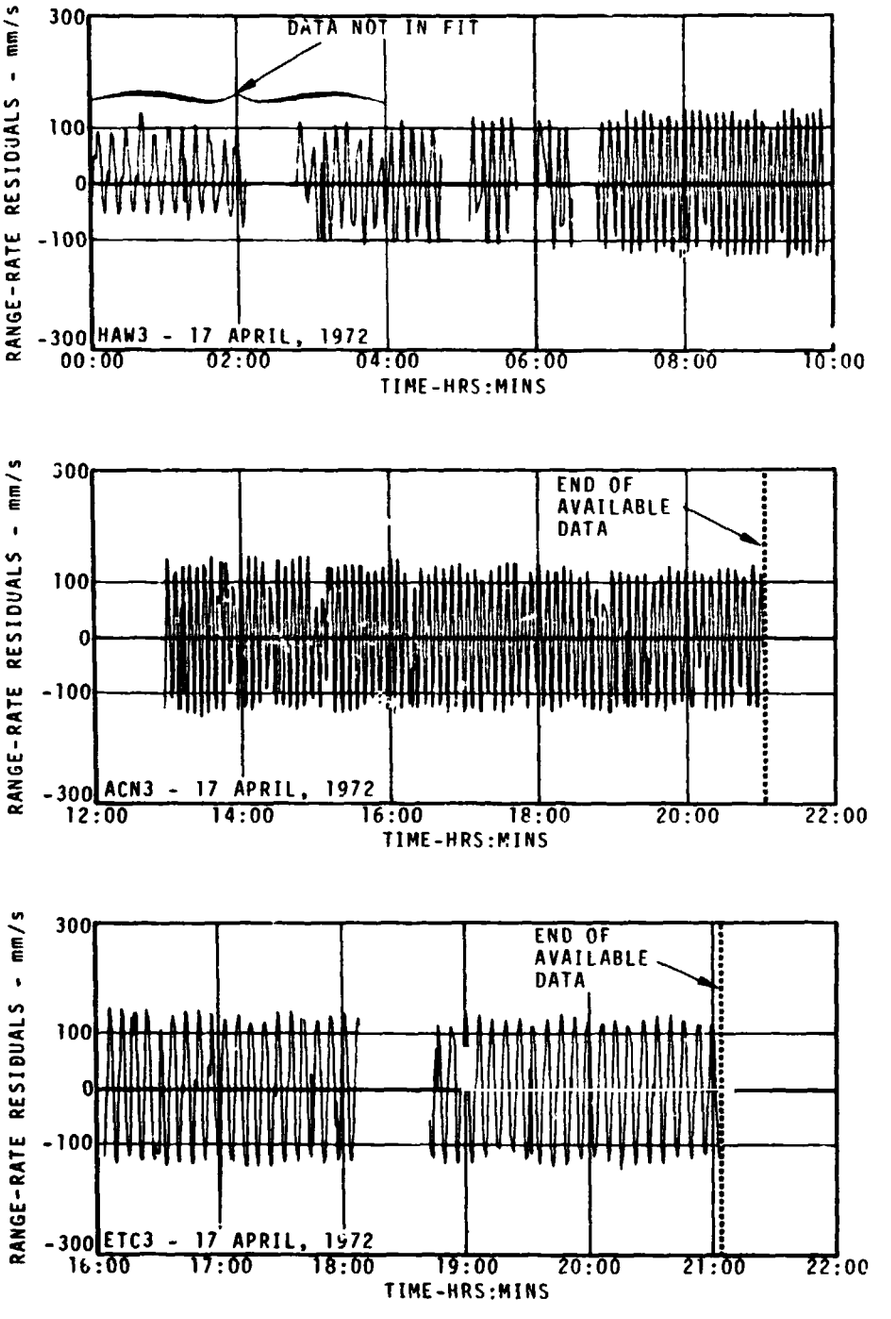

FIGURE 3-8. HAWAII, ASCENSION, AND GREENBELT RANGE-RATE RESIDUALS FOR LATE PTC DATA FIT/BEST-ESTIMATE TRAJECTORY

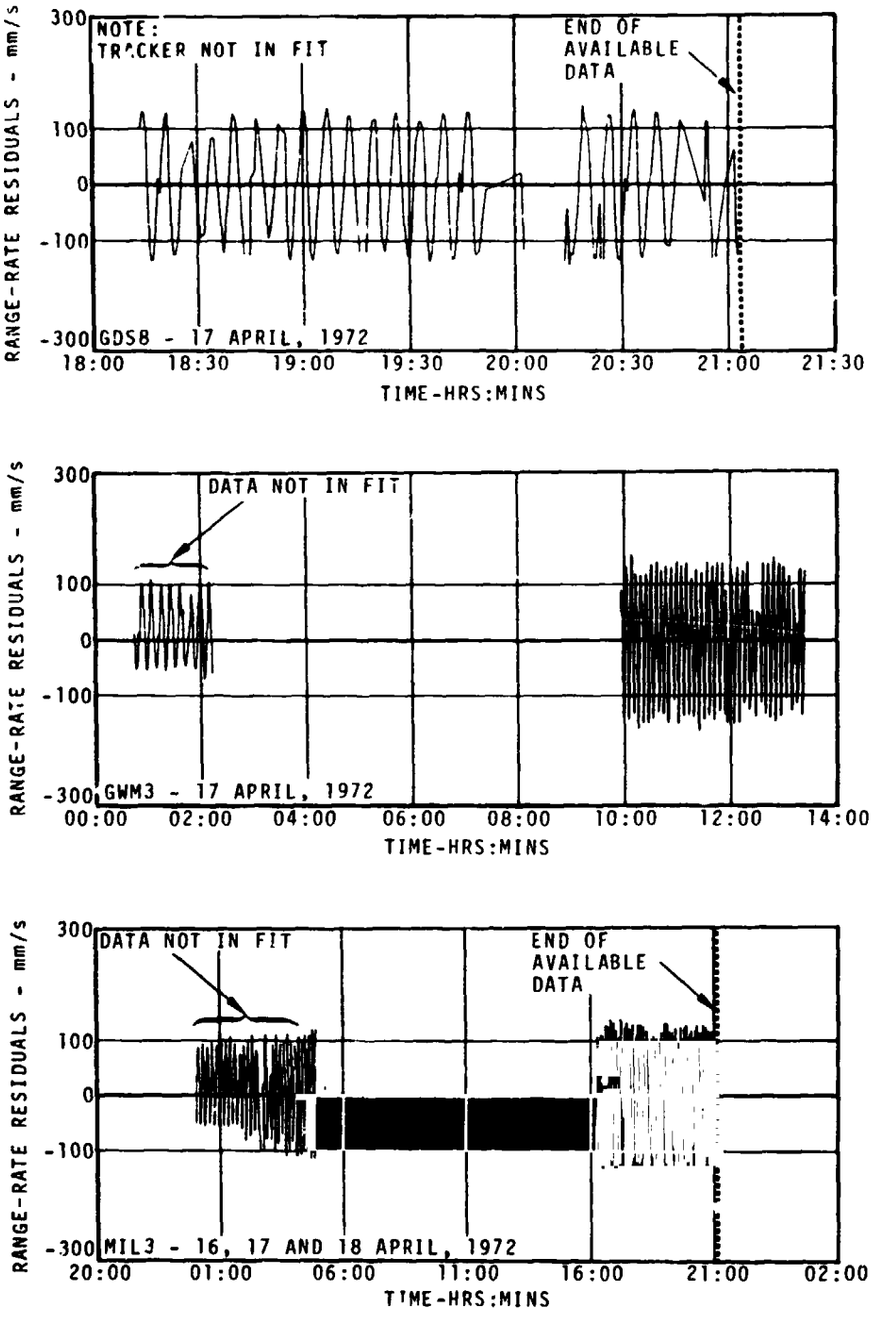

FIGURE 3-9. GOLDSTONE, GUAM, AND MERRITT ISLAND RANGE-RATE RESIDUALS FOR LATE PTC DATA FIT/BEST-ESTIMATE TRAJECTORY

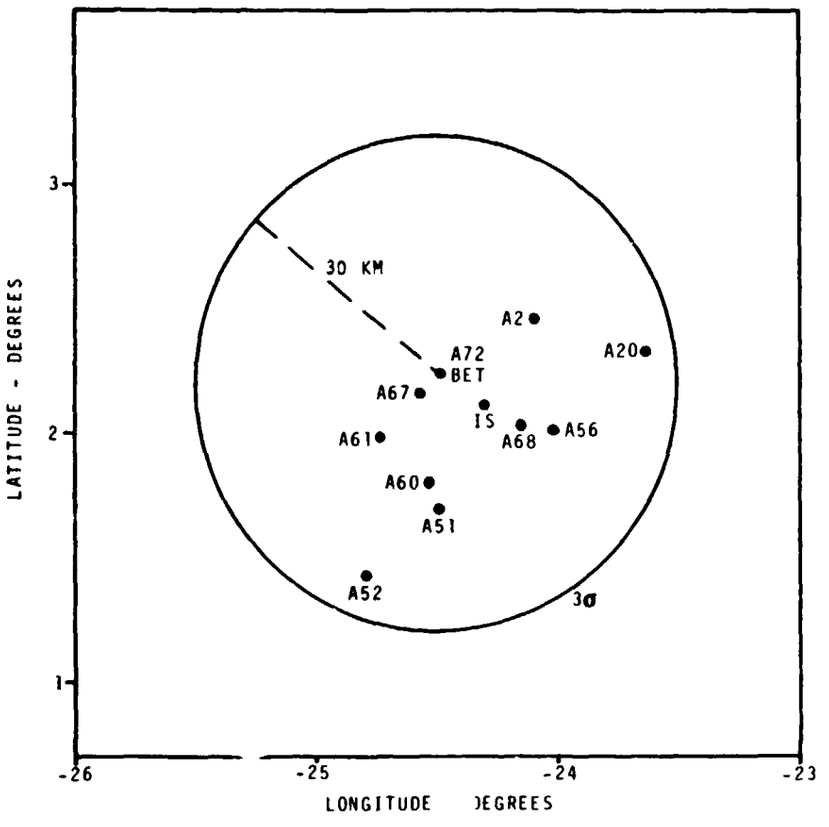

LEGEND:

BET	- BEST ESTIMATE TRAJECTORY POINT (A72)
IS	- POINT CALCULATED FROM SEISMIC DATA
OTHER POINTS	- BASED ON DIFFERENT COMBINATIONS OF TRACKING DATA AND NON-GRAVITATIONAL ACCELERATIONS
3σ CIRCLE	- ESTIMATE BASED ON DISTRIBUTION OF SOLUTIONS AND MODEL ERRORS

FIGURE 3-10. DISTRIBUTION OF LUNAR IMPACT SOLUTIONS

TABLE 3-I. TRACKING STATION LOCATIONS

ABBREVIATION	STATION	LOCATION			CONFIGURATION
		LATITUDE	LONGITUDE	HEIGHT	
MADW	Madrid, Spain	40°25'41.85"	355°45'03.62"	767m	DSN 85' S-Band
GDSW	Goldstone, California	35°23'22.45"	243°09'02.26"	985m	DSN 85' S-Band
GDS8	Goldstone, California	35°20'29.74"	243°07'35.05"	921m	STDN 85' S-Band
HSKW	Tidbinbilla, Australia	-35°24'03.56"	148°58'52.65"	669m	DSN 85' S-Band
ACN3	Ascension	- 7°57'17.26"	345°40'22.59"	527m	STDN 30 S-Band
BDA3	Bermuda	32°21'04.50"	295°20'31.93"	-43m	STDN 30' S-Band
ETC3	Greenbelt, Maryland	38°59'54.53"	283°09'25.51"	-22m	STDN 30' S-Band
MIL3	Merritt Island, Florida	28°30'29.78"	279°18'23.51"	-54m	STDN 30' S-Band
HAW3	Kauai, Hawaii	22°07'34.71"	200°20'05.42"	1143m	STDN 30' S-Band
GWM3	Guam	13°18'38.07"	144°44'12.54"	114m	STDN 30' S-Band
CRO3	Carnarvon, Australia	-24°54'23.68"	113°43'32.06"	5m	STDN 30' S-Band
BDQC	Bermuda	32°20'52.54"	295°20'47.91"	-45m	STDN FPQ-6 C-Band
MILC	Merritt Island, Florida	28°25'29.48"	279°20'07.96"	-53m	STDN TPQ-18 C-Band

*Height above Fischer Ellipsoid

TABLE 3-II. PRE-PTC TRAJECTORY SEGMENT - DATA UTILIZATION AND RESIDUAL STATISTICS

	RANGE-RATE RESIDUAL STATISTICS				
STATION	TIME ARC 16 APRIL HR:MIN	NUMBER OF POINTS	MEAN, mm/s	SIGMA, mm/s	RMS, mm/s
GDSW	21:12 to 23:48	103	-4	13	14
ETC3	22:50 to 23:47	30	-15	8	17
BDA3	21:12 to 22:00	67	0	7	7
MIL3	21:12 to 23:48	99	-1	12	12
HAW3	21:12 to 23:47	92	-1	16	16
	RANGE RESIDUAL STATISTICS				
STATION	TIME ARC 16 APRIL HR:MIN	NUMBER OF POINTS	MEAN, M	SIGMA, M	RMS, M
BDQC	21:12 to 23:48	156	-2	20	20
MILC	21:12 to 23:48	156	-1	29	29

TABLE 3-III. LATE PTC TRAJECTORY SEGMENT - DATA UTILIZATION AND RESIDUAL STATISTICS/ BEST-ESTIMATE TRAJECTORY

	BET RANGE-RATE RESIDUAL STATISTICS				
STATION	TIME ARC 17 APRIL HR:MIN	NUMBER OF POINTS	MEAN, mm/s	SIGMA, mm/s	RMS, mm/s
MADW	10:55 to 21:04	544	0.6	93.7	93.7
GDSW	4:00 to 6:48	155	-1.4	79.8	79.8
HSKW	4:00 to 11:16	421	-0.6	89.0	89.0
ETC3	16:04 to 21:04	243	2.7	89.4	89.5
ACN3	12:56 to 21:04	433	0.4	90.8	90.8
MIL3	4:00 to 4:56	74	1.5	73.6	73.6
	16:13 to 21:04	249	2.1	85.0	85.0
HAW3	4:00 to 9:52	245	7.1	86.3	86.6
GWM3	9:55 to 13:26	194	0.2	98.3	98.3
	BET RANGE RESIDUAL STATISTICS				
STATION	TIME ARC 17 APRIL HR:MIN	NUMBER OF POINTS	MEAN, M	SIGMA, M	RMS, M
MADW	10:56 to 20:56	101	0.1	9.3	9.3
HSKW	4:58 to 10:46	48	-0.3	10.2	10.2
GDSW	2:18 to 4:49	14	-1.7	17.6	17.7

TABLE 3-IV. LATE PTC TRAJECTORY SEGMENT - DATA UTILIZATION AND RESIDUAL STATISTICS/ BEST GRAVITATIONAL TRAJECTORY

	RUN A20 RANGE-RATE RESIDUAL STATISTICS				
STATION	TIME ARC 17 APRIL HR:MIN	NUMBER OF POINTS	MEAN, mm/s	SIGMA, mm/s	RMS, mm/s
MADW	10:55 to 21:04	525	1	94	94
GDSW	4:00 to 6:48	155	13	80	81
HSKW	4:00 to 11:16	421	0	90	90
ETC3	16:04 to 21:04	243	11	89	90
ACN3	12:56 to 21:04	433	0	91	91
MIL3	16:13 to 21:04	248	-13	98	99
HAW3	4:00 to 9:52	245	7	88	88
GWM3	9:55 to 13:26	194	-13	98	99
	RUN A20 RANGE RESIDUAL STATISTICS				
STATION	TIME ARC 17 APRIL HR:MIN	NUMBER OF POINTS	MEAN, M	SIGMA, M	RMS, M
MADW	10:56 to 20:56	101	0	12	12
HSKW	4:58 to 10:46	48	0	35	35

TABLE 3-V. TRAJECTORY SOLUTIONS AND LUNAR IMPACT POINTS

RUN ID	LATITUDE, LONGITUDE TIME, 19 APRIL	NON-GRAVITATIONAL ACCELERATION ARC, 17 APRIL	DESCRIPTION
A2	2.47° -24.09° 21:01:39	None	MADW, ETC3, ACN3, and MIL3 range rate after 18:00:00 April 17 plus MADW range after 18:00:00 April 17
A20	2.33° -23.63° 21:01:21	None	MADW, GDSW, HSKW, ETC3, ACN3, MIL3, HAW3, and GWM3 range rate after 04:00:00 April 17 plus MADW and HSKW range after 04:00:00 April 17
A51	1.69° -24.49° 21:01:54	4:00:00 to 18:00:00	MADW, GDSW HSKW, ETC3, ACN3, MIL3, and HAW3 range rate after 04:00:00 April 17 plus MADW and HSKW range after 04:00:00
A52	1.43° -24.79° 21:02:06	4:00:00 to 21:00:00	Same as A51
A56	2.02° -24.03° 21:01:36	4:00:00 to 12:00:00	Same as A51
A60	1.80° -24.53° 21:01:56	4:00:00 to 16:00:00	MADW, GDSW, GDS8, HSKW, ETC3, ACN3 MIL3, HAW3, and GWM3 range rate after 4:00:00 April 17 plus MADW, GDSW, and HSKW range after 4:00:00 April 17
A61	1.98° -24.73° 21:02:04	4:00:00 to 16:00:00	Same as A51
A67	2.16° -24.56° 21:01:58	4:00:00 to 12:00:00	MADW, GDSW, HSKW, ETC3, ACN3, MIL3, and HAW3 range rate after 4:00:00 April 17; MADW and HSKW range after 4:00:00 April 17 plus BDQC range from 0:00:00 April 17 to 4:00:00 April 17
A68	2.04° -24.15° 21:01:41	2:00:00 to 12:00:00	MADW, GDSW, HSKW, ETC3, ACN3, MIL3, and HAW3 range rate after 2:00:00 April 17 plus MADW, HSKW, MIL3, GDSW, BDQC range after 0:00:00 April 17
A72 (BET)	2.24° -24.49° 21:01:55	4:00:00 to 12:00:00	MADW, GDSW, HSKW, ETC3, ACN3, MIL3, HAW3 and GWM3 range after 4:00:00 April 17 plus MADW, GDSW and HSKW range after 2:00:00 April 17
MEAN/ SIGMA	1.98°/0.29° -24.44°/0.27° 21:01:50/10^{s}	Run A20 not in statistics	

TABLE 3-VI. APOLLO 16 LUNAR IMPACT SEISMIC DATA

SEISMOMETER	LOCATION		IMPACT SIGNAL RECEPTION TIME 19 APRIL HR:MIN:SEC
	LATITUDE deg	LONGITUDE deg	
Apollo 12	-3.04	-23.42	21:02:32
Apollo 14	-3.67	-17.47	21:02:40
Apollo 15	26.07	3.65	21:04:30

The derived Apollo 16 S-IVB/IU impact conditions, calculated by the principal seismic investigator based upon above data, are 2.1° latitude, -24.3° longitude, and 21:02:02, April 19, 1972.

APPENDIX A

ANALYSIS METHODS

The trajectories reconstructed for this analysis are based on tracking data and onboard measurements by the S-IVB/IU. Goddard Space Flight Center is the central collection agency for all tracking data recorded by the Manned Space Flight Network tracking stations. This data is transmitted to The Boeing Company via Marshall Space Flight Center in the form of two angles and range measurements and, in the case of S-band data, in the form of doppler counts. Onboard measurements in the form of platform attitudes and velocity accumulations are collected by the Marshall Space Flight Center and transmitted to The Boeing Company. Trajectory determination is accomplished by:

a. Propagating an a priori initial state forward by means of an a priori acceleration model.

b. Transformation of the propagated initial state (the trajectory) into tracking observations.

c. Converting the difference in the observed tracking data and the calculated tracking data into an estimate of the correction to the initial state.

This appendix briefly summarizes the three steps outlined above as implemented in the Lunar Impact Determination (LID) program (see Reference 3). The LID program, originally received from MSFC, was modified by The Boeing Company in several ways. First, the program was converted to run on an IBM 360/370 and was made double-precision. Second, computer graphics capability was added to provide a quick-response man/machine interface for on-line decision making. Finally, numerous improvements were made in the model which transforms the trajectory into tracking data, and the capability to solve for non-gravitational acceleration was added.

A.1 INITIAL STATE PROPAGATION

Initial state propagation is accomplished by numerical integration of an acceleration model which consists of the gravitational attractions of the earth, moon, and sun, plus non-gravitational accelerations.

The earth's gravitational potential is expressed in the J, D, H form; the moon's includes the second zonal and second

A.1 (Continued)

sectoral harmonics. Details of the expansions, and the coefficients used, are given in Reference 3. The ephemeris used is the JPL ephemeris DE19, transformed to PACSS4 coordinates (Reference 4) by the Manned Spacecraft Center. The ephemeris time to universal time correction used is 42.35 seconds. The non-gravitational acceleration is a square wave time history input via cards. The acceleration history is derived from platform data or other sources. The total acceleration is the sum of gravitational and non-gravitational acceleration:

$$\vec{A} = \vec{G} + \vec{T}.$$

The non-gravitational acceleration is calculated as follows:

$$\vec{T} = [B]\vec{T}_o \qquad \text{if } t < t_s \text{ or } t_e < t,$$

or

$$\vec{T} = [B](\vec{C}'_o + [C''_o]\vec{T}_o + \vec{T}_o) \qquad \text{if } t_s \leq t \leq t_e;$$

where $\vec{T}_o$ is the initial a priori time history of the thrust accelerations,

$\vec{C}'_o$ is the a priori thrust bias vector,

$[C''_o]$ is a diagonal matrix where the diagonal terms are the a priori thrust scale factors,

$[B]$ is a transformation matrix relating PACSS13 to PACSS4,

t_s is the start of the window over which corrections are made to the thrust history,

t_e s the end of the window over which corrections are made to the thrust history,

and t is the current time.

A.2 CALCULATION OF OBSERVABLES

Tracking observations are calculated by determining the instantaneous tracker position and velocity in the reference system and examining the relationship of the vehicle to the tracker. This examination includes consideration of signal travel time and atmospheric refraction. A summary of the calculation of observables is presented below. Figure A-1 will help in understanding the equations.

A.2 (Continued)

Define: t_4 = time of signal reception at tracker, also time tag of observation;

t_3 = time of signal transmission from vehicle;

t_2 = time of signal reception at vehicle;

t_1 = time of signal transmission from tracker.

From the vehicle trajectory:

$\vec{P}_V^4$ = position of vehicle at t_4; and

$\vec{V}_V^4$ = velocity of vehicle at t_4.

The tracker position(s)

$\vec{P}_T^4$ (the position of transmitting tracker at t_4) and

$\vec{P}_R^4$ (the position of receiving tracker at t_4)

are determined as follows:

$$\vec{P}_T^4 = [P][N][R]\vec{R}_T, \text{ and}$$

$$\vec{P}_R^4 = [P][N][R]\vec{R}_R;$$

where

$\vec{R}_T$ and $\vec{R}_R$ are the earth fixed position(s) of the tracker(s),

[R] is the matrix modeling the earth's rotation,

[N] is the matrix modeling the earth's nutation,

[P] is the matrix modeling the earth's precession.

Note that [R], [N], and [P] are time dependent.

The following nomenclature is introduced:

c is the speed of light;

δ is the vehicle transponder delay distance, (apparent distance from receiving antenna to transmitting antenna);

A.2 (Continued)

ω is earth spin rate; and

n is atmospheric refraction coefficient ($n = (\eta-1)(10^6)$ where η is the index of refraction).

Calculation of downlink distance, d":

$$\left.\begin{aligned} d'' &= |\vec{P}_V^4 - \vec{P}_R^4| \\ \vec{P}_V^3 &= \vec{P}_V^4 - \frac{d''}{c}\,\vec{V}_V^4 \\ \vec{P}^{34} &= \vec{P}_R^4 - \vec{P}_V^3 \\ d'' &= |\vec{P}^{34}| \end{aligned}\right\} \text{ iterated twice}$$

Calculation of elevation:

$$e = \sin^{-1}\left(\frac{\vec{P}^{34} \cdot \vec{P}_T^4}{d''\ |\vec{P}_T^4|}\right).$$

Calculation of downlink distance refraction correction:

$$\Delta d'' = \left(\frac{0.00118958}{(0.06483 + \sin e)^{1.4}}\right)\left(\frac{n}{340}\right), \qquad e \leq 15^\circ$$

$$\Delta d'' = \left(\frac{0.0026}{0.015 + \sin e}\right)\left(\frac{n}{340}\right), \qquad e > 15^\circ$$

$d'' = d'' + \Delta d''$, (see Reference 5).

Calculation of uplink distance, d':

$$\vec{P}_V^2 = \vec{P}_V^3 - \frac{\delta}{c}\,\vec{V}_V^4$$

$$\vec{V}_T^4 = \left[[P][N]\begin{bmatrix}0\\0\\\omega\end{bmatrix}\right] \times \vec{P}_T^4$$

$d' = d''$

A.2 (Continued)

$$\left.\begin{aligned} \vec{P}_T^1 &= \vec{P}_T^4 - \frac{d' + d'' + \delta}{c}\vec{V}_T^4 \\ \vec{P}^{12} &= \vec{P}_V^2 - \vec{P}_T^1 \\ d' &= |\vec{P}^{12}|. \end{aligned}\right\} \quad \begin{array}{l} \text{2 way tracking-iterated once} \\ \text{3 way tracking-iterated twice} \end{array}$$

Calculation of uplink distance refraction correction:

$$d' = d' + \Delta d'', \qquad \text{if 2 way, or if 3 way}$$

$$e' = \sin^{-1}\left(\frac{\vec{P}^{12} \cdot \vec{P}_T^1}{d' \, |\vec{P}_T^1|}\right)$$

$$d' = d' + \left(\frac{0.00118958}{(0.06483 + \sin e')^{1.4}}\right)\left(\frac{n}{340}\right), \quad e' \leq 15°$$

$$d' = d' + \left(\frac{0.0026}{0.015 + \sin e'}\right)\left(\frac{n}{340}\right), \qquad e' > 15°.$$

Calculation of range:

$$\rho = \frac{1}{2}(d'' + d' + \delta).$$

Calculation of average range rate:

$$\dot{\rho} = \frac{\rho - \rho^*}{t_4 - t_4^*}, \qquad *\text{indicates previous value.}$$

A.3 CORRECTION OF INITIAL STATE

The LID program uses Kalman estimation techniques (described in Reference 6) to correct an initial state consisting of the initial position, initial velocity, thrust acceleration biases, and thrust acceleration scale factors. For simplicity of notation let

$\vec{C}_o = (\vec{C}_o', \vec{C}_o'')^T$, a six element vector with $\vec{C}_o''$ representing the diagonal terms of $[C_o'']$,

$\vec{S}_o = (\vec{P}_o, \vec{V}_o)^T$, a six element vector,

A.3 (Continued)

and $\vec{S}^*_o = (\vec{S}_o, \vec{C}_o)^T$, a twelve element vector.

The Kalman Optimal Estimation technique adapted to solve for corrections to the extended initial state is given below.

Assume that there exists a first guess to the initial state and an estimate of its uncertainty, then the correction to the initial state, $\hat{S}^*_o$, which results in the best fit of a set of measurements is given by:

$$\hat{S}^*_{o,j} = \hat{S}^*_{o,j-1} + K_j(Y_j - H_j\phi_j\hat{S}^*_{o,j-1}), \text{ with}$$

$$K_j = P_{j-1}\phi_j^T H_j^T (H_j\phi_j P_{j-1}\phi_j^T H_j^T + Q_j)^{-1}, \text{ and}$$

$$P_j = P_{j-1} - K_j H_j \phi_j P_{j-1};$$

where $\hat{S}^*_{o,j}$ is the correction matrix (12 × 1) to the initial state at time j,

K_j is the Kalman gain matrix (12 × 1) at time j,

Y_j is the measurement matrix (1 × 1) at time j perturbed by noise,

H_j is the matrix (1 × 6) relating, at time j, the measurement matrix to the propagated initial state,

ϕ_j is the transition matrix (6 × 12) relating, at time j, changes in the propagated initial state to changes in the initial state,

P_j is the covariance matrix (12 × 12), at time j, of the perturbations to the initial state,

and Q_j is the covariance matrix (1 × 1) of the error in the measurements at time j.

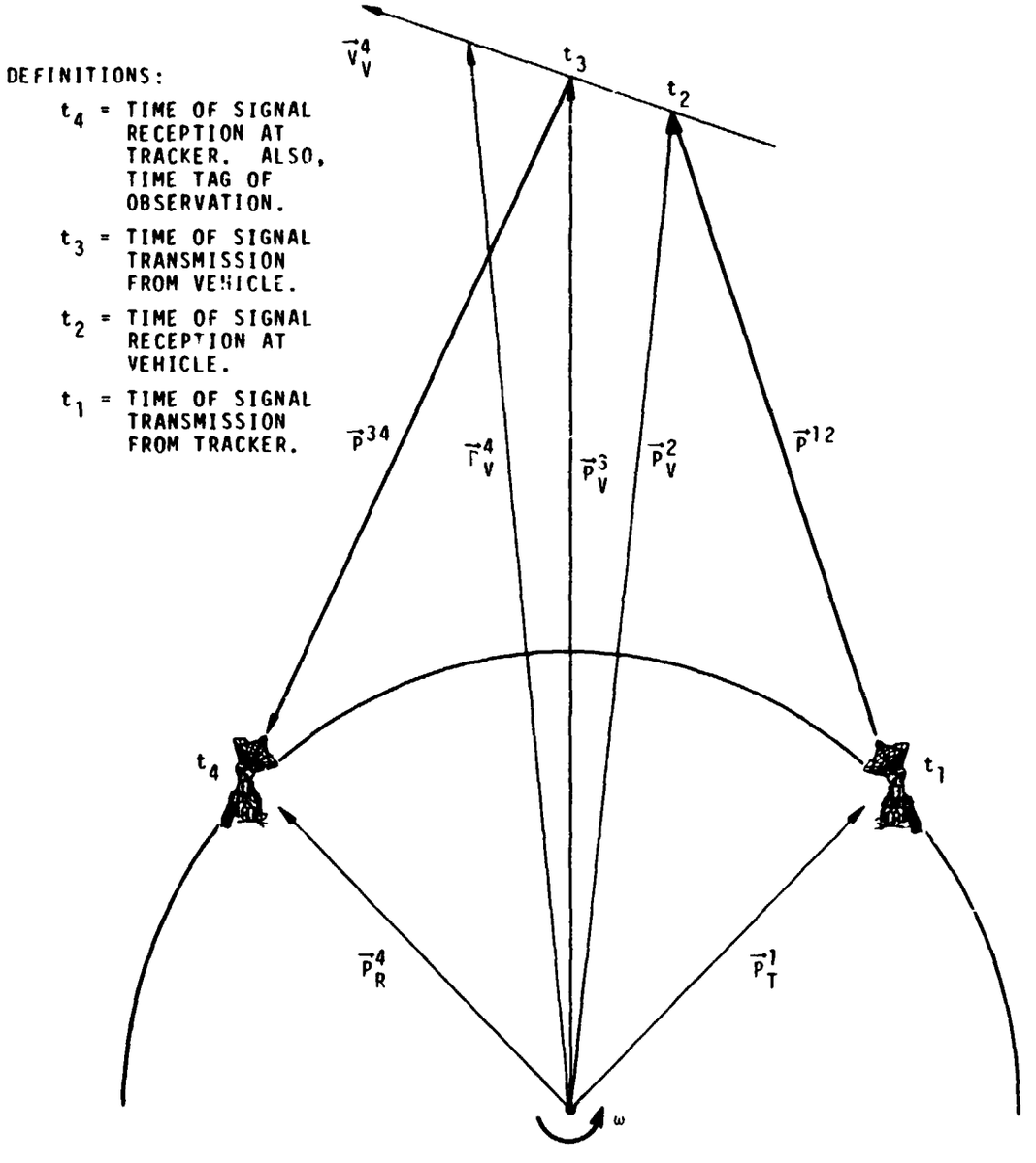

FIGURE A-1. DIAGRAM FOR USB RANGE CALCULATION

THIS PAGE LEFT BLANK INTENTIONALLY

APPENDIX B

BEST-ESTIMATE TRAJECTORY HISTORY

This appendix contains a time history of the composite best-estimate AS-511 lunar impact trajectory from CSM/LV separation to lunar impact. The following parameters are included:

1. Greenwich Mean Time in hours, minutes, and seconds.

2. Time from beginning of the launch day in hours.

3. PACSS4 (MNBY) position in kilometers and velocity in kilometers per second.

4. Declination and longitude in degrees, both geocentric and selenocentric.

5. The following selected osculating orbital elements relative to either the earth or moon.

   a. Semi-major axis in kilometers (orbit is hyperbolic when negative).

   b. Eccentricity.

   c. Inclination in degrees.

   d. Right ascension of ascending node in degrees.

   e. Argument of perifocus in degrees.

   f. True anomaly in degrees.

The trajectory from CSM separation to 24:00:00, April 16, 1972, was generated using the non-gravitational accelerations given in Table 2-II. The trajectory from 06:00:00, April 17, 1972, to lunar impact was generated using non-gravitational accelerations of

$$-13.82309130 \times 10^{-6} \text{ m/s}^2$$
$$-4.14591928 \times 10^{-6} \text{ m/s}^2$$
$$5.97387629 \times 10^{-6} \text{ m/s}^2$$

until 12:00:00, April 17, 1972.

These accelerations and the accelerations of Table 2-II are expressed in PACSS13. The transformation of any vector from PACSS13 to PACSS4 (MNBY) is given by

APPENDIX B (Continued)

$$\vec{V}_4 = [B]\vec{V}_{13}$$

where

$$[B] = \begin{bmatrix} 0.7380782287080494 & 0.2158384602954925 & -0.6392607349147001 \\ 0.4754163491357247 & 0.5059341917359541 & 0.7197290380796192 \\ 0.4787690701884745 & -0.8351313392663046 & 0.2709058784393385 \end{bmatrix}$$

The gravitational effects of the earth, moon and sun were included. Trajectory integration was carried out in double precision and is based on a DE19 ephemeris with a time correction of 42.35 seconds. The lunar impact analysis wa conducted on IBM 360 Model 44, IBM 360 Model 65, and IBM 3 Model 155 computers.

S-IVB LUNAR-IMPACT TRAJECTORY (CONTINUED)

16 APRIL 1972 G.M.T. = 20 HR 58 MIN 59.000000 SEC

TIME = 20.98306

CSM/LV SEPARATED

PARAMETER	GEOCENTRIC	SELENOCENTRIC
X -	1.1004023880 04	-1.1473128480 05
Y -	5.1951315220 03	-2.9696688320 05
Z -	5.9418572560 03	-1.5209772350 05
|R| -	1.3541920130 04	3.5282617800 05
XD -	1.5211396250 00	2.5133359100 00
YD -	6.2327830760 00	5.8205641090 00
ZD -	4.0113282100 00	3.8931975430 00
|V| -	7.5665186610 00	7.4399469790 00
DECLINATION -	2.6029177560 01	-4.6225490810 00
LONGITUDE -	-1.3456182670 02	6.0991136980 00
SEMI-MAJOR AXIS -	2.4645907560 05	
ECCENTRICITY -	0.9732950330 00	
INCLINATION -	3.2501695870 01	
RIGHT ASC. OF NODE -	-2.4763190210 01	
ARG. OF PERIFOCUS -	-3.7655358410 01	
TRUE ANOMALY -	9.2410388230 01	

S-IVB LUNAR-IMPACT TRAJECTORY (CONTINUED)

16 APRIL 1972 G.M.T. = 21 HR 0 MIN 0.0 SEC

TIME = 21.00000

PARAMETER	GEOCENTRIC	SELENOCENTRIC
X -	1.109359631D 04	-1.145811865D 05
Y -	5.5737801610 03	-2.9661337520 05
Z -	6.1847912250 03	-1.5186199300 05
|R| -	1.3870347750 04	3.5237821230 05
XD -	1.4167708020 00	2.4090301340 00
YD -	6.1819395330 00	5.7698754270 00
ZD -	3.9540236540 00	3.8359740540 00
|V| -	7.4738155550 00	7.3355017260 00
DECLINATION -	2.6484370910 01	-4.6146374170 00
LONGITUDE -	-1.3341277680 02	6.0906052470 00
SEMI-MAJOR AXIS -	2.4640581330 05	
ECCENTRICITY -	0.9732893090 00	
INCLINATION -	3.2501485130 01	
RIGHT ASC. OF NODE -	-2.4763759420 01	
ARG. OF PERIFOCUS -	-3.7655155730 01	
TRUE ANOMALY -	9.3749473680 01	

S-IVB LUNAR-IMPACT TRAJECTORY (CONTINUED)

16 APRIL 1972 G.M.T. = 21 HR 15 MIN 53.000000 SEC

TIME = 21.26472

CSM/LM DOCKED

PARAMETER	GEOCENTRIC	SELENOCENTRIC
X -	1.187822640D 04	-1.128504648D 05
Y -	1.110802161D 04	-2.914706784D 05
Z -	9.595240405D 03	-1.485634419D 05
|R| -	1.888250632D 04	3.460657123D 05
XD -	3.774665461D-01	1.370706644D 00
YD -	5.461815047D 00	5.052171498D 00
ZD -	3.259712199D 00	3.142929311D 00
|V| -	6.371783755D 00	6.105839680D 00
DECLINATION -	3.054425236D 01	-4.516314421D 00
LONGITUDE -	-1.209894304D 02	5.889752291D 00
SEMI-MAJOR AXIS -	2.460995930D 05	
ECCENTRICITY -	0.973256214D 00	
INCLINATION -	3.249960947D 01	
RIGHT ASC. OF NODE -	-2.477084212D 01	
ARG. OF PERIFOCUS -	-3.765065651D 01	
TRUE ANOMALY -	1.087104798D 02	

S-IVB LUNAR-IMPACT TRAJECTORY (CONTINUED)

16 APRIL 1972 G.M.T. = 21 HR 53 MIN 15.000000 SEC

TIME = 21.88750

CSM/LM EJECTED

PARAMETER	GEOCENTRIC	SELENOCENTRIC
X -	1.160495751D 04	-1.108943285D 05
Y -	2.202762400D 04	-2.814631079D 05
Z -	1.583757556D 04	-1.425795929D 05
|R| -	2.950796598D 04	3.344367971D 05
XD -	-4.300198689D-01	5.564961928D-01
YD -	4.395813252D 00	3.991872842D 00
ZD -	2.425014373D 00	2.311213067D 00
|V| -	5.039504668D 00	4.646121247D 00
DECLINATION -	3.246346350D 01	-4.380353974D 00
LONGITUDE -	-1.112187815D 02	5.213526364D 00
SEMI-MAJOR AXIS -	2.460448120D 05	
ECCENTRICITY -	0.973250539D 00	
INCLINATION -	3.249897822D 01	
RIGHT ASC. OF NODE -	-2.477677258D 01	
ARG. OF PERIFOCUS -	-3.764630963D 01	
TRUE ANOMALY -	1.251183304D 02	

S-IVB LUNAR-IMPACT TRAJECTORY (CONTINUED)

16 APRIL 1972 G.M.T. = 22 HR 0 MIN 0.0 SEC

TIME = 22.00000

PARAMETER	GEOCENTRIC	SELENOCENTRIC
X -	1.1413222070 04	-1.1068279740 05
Y -	2.3780871670 04	-2.7987324770 05
Z -	1.6800254520 04	-1.4166289450 05
|R| -	3.1273631810 04	3.3263807640 05
XD -	-5.0552724950-01	4.9039525320-01
YD -	4.2641959160 00	3.8612870060 00
ZD -	2.3309162520 00	2.2176537690 00
|V| -	4.8859078160 00	4.4797335950 00
DECLINATION -	3.2495973860 01	-4.3630380250 00
LONGITUDE -	-1.1076681540 02	5.0813235240 00
SEMI-MAJOR AXIS -	2.4616796120 05	
ECCENTRICITY -	0.9732585870 00	
INCLINATION -	3.2498792200 01	
RIGHT ASC. OF NODE -	-2.4785049010 01	
ARG. OF PERIFOCUS -	-3.7632554570 01	
TRUE ANOMALY -	1.2692052910 02	

S-IVB LUNAR-IMPACT TRAJECTORY (CONTINUED)

16 APRIL 1972 G.M.T. = 22 HR 12 MIN 8.000000 SEC

TIME = 22.20222

APS EVASIVE BURN INITIATED

PARAMETER	GEOCENTRIC	SELENOCENTRIC
X -	1.1009735180 04	-1.1036098730 05
Y -	2.6807450980 04	-2.7713931160 05
Z -	1.8442718020 04	-1.4010253380 05
|R| -	3.4350946750 04	3.2956708500 05
XD -	-5.9806109060-01	3.9858838950-01
YD -	4.0561894480 00	3.6551356550 00
ZD -	2.1858964800 00	2.0736027120 00
|V| -	4.6463419300 00	4.2212222840 00
DECLINATION -	3.2474731910 01	-4.3352684850 00
LONGITUDE -	-1.1049828130 02	4.8409082350 00
SEMI-MAJOR AXIS -	2.4617220280 05	
ECCENTRICITY -	0.9732590760 00	
INCLINATION -	3.2498797120 01	
RIGHT ASC. OF NODE -	-2.4785854660 01	
ARG. OF PERIFOCUS -	-3.7631876320 01	
TRUE ANOMALY -	1.2971272460 02	

S-IVB LUNAR-IMPACT TRAJECTORY (CONTINUED)

16 APRIL 1972 G.M.T. = 22 HR 28 MIN 47.000000 SEC

TIME = 22.47972

CVS VENT INITIATED

PARAMETER	GEOCENTRIC	SELENOCENTRIC
X -	1.036744288D 04	-1.100071309D 05
Y -	3.073643526D 04	-2.736097088D 05
Z -	2.054068772D 04	-1.381160819D 05
|R| -	3.839442895D 04	3.256376696D 05
XD -	-6.844440365D-01	3.131954820D-01
YD -	3.817579622D 00	3.419073520D 00
ZD -	2.022171624D 00	1.911207519D 00
|V| -	4.373963407D 00	3.929487158D 00
DECLINATION -	3.234564686D 01	-4.302984718D 00
LONGITUDE -	-1.109836089D 02	4.508421303D 00
SEMI-MAJOR AXIS -	2.442361948D 05	
ECCENTRICITY -	0.973109412D 00	
INCLINATION -	3.250127934D 01	
RIGHT ASC. OF NODE -	-2.490157942D 01	
ARG. OF PERIFOCUS -	-3.761056518D 01	
TRUE ANOMALY -	1.329055434D 02	

S-IVB LUNAR-IMPACT TRAJECTORY (CONTINUED)

16 APRIL 1972 G.M.T. = 22 HR 33 MIN 27.000000 SEC

TIME = 22.55750

LOX DUMP INITIATED

PARAMETER	GEOCENTRIC	SELENOCENTRIC
X -	1.0173050280 04	-1.0992214570 05
Y -	3.1796963280 04	-2.7266066280 05
Z -	2.1101287910 04	-1.3758649960 05
|R| -	3.9494330930 04	3.2458705800 05
XD -	-7.0373832570-01	2.9417711190-01
YD -	3.7581181850 00	3.3603265630 00
ZD -	1.9824921720 00	1.8719008130 00
|V| -	4.3068521150 00	3.8577645650 00
DECLINATION -	3.2297818310 01	-4.2948742870 00
LONGITUDE -	-1.1125556490 02	4.4149722430 00
SEMI-MAJOR AXIS -	2.4359102750 05	
ECCENTRICITY -	0.9730438650 00	
INCLINATION -	3.2501660170 01	
RIGHT ASC. OF NODE -	-2.4908697720 01	
ARG. OF PERIFOCUS -	-3.7614756850 01	
TRUE ANOMALY -	1.3367602480 02	

S-IVB LUNAR-IMPACT TRAJECTORY (CONTINUED)

16 APRIL 1972 G.M.T. = 23 HR 0 MIN 0.0 SEC

TIME = 23.00000

PARAMETER	GEOCENTRIC	SELENOCENTRIC
X -	8.985833772D 03	-1.095184390D 05
Y -	3.753472493D 04	-2.675533454D 05
Z -	2.409565786D 04	-1.347666131D 05
|R| -	4.549946713D 04	3.189688381D 05
XD -	-7.817232014D-01	2.177489418D-01
YD -	3.464137965D 00	3.070414623D 00
ZD -	1.790325690D 00	1.681855544D 00
|V| -	3.977010068D 00	3.507634335D 00
DECLINATION -	3.197924031D 01	-4.255051752D 00
LONGITUDE -	-1.136329690D 02	3.884960575D 00
SEMI-MAJOR AXIS -	2.338375449D 05	
ECCENTRICITY -	0.972030693D 00	
INCLINATION -	3.250567205D 01	
RIGHT ASC. OF NODE -	-2.497759947D 01	
ARG. OF PERIFOCUS -	-3.773341075D 01	
TRUE ANOMALY -	1.374892062D 02	

S-IVB LUNAR-IMPACT TRAJECTORY (CONTINUED)

16 APRIL 1972 G.M.T. = 23 HR 34 MIN 7.000000 SEC

TIME = 23.56861

APS IMPACT BURN INITIATED

PARAMETER	GEOCENTRIC	SELENOCENTRIC
X -	7.320922340D 03	-1.091354093D 05
Y -	4.432293751D 04	-2.615657295D 05
Z -	2.756809634D 04	-1.315134232D 05
|R| -	5.270786114D 04	3.124467120D 05
XD -	-8.388504416D-01	1.625893985D-01
YD -	3.181173883D 00	2.792686622D 00
ZD -	1.611513845D 00	1.505770765D 00
|V| -	3.663402000D 00	3.176929252D 00
DECLINATION -	3.153799089D 01	-4.214995891D 00
LONGITUDE -	-1.181011705D 02	3.209076936D 00
SEMI-MAJOR AXIS -	2.338553935D 05	
ECCENTRICITY -	0.972033246D 00	
INCLINATION -	3.250578728D 01	
RIGHT ASC. OF NODE -	-2.497864837D 01	
ARG. OF PERIFOCUS -	-3.773267275D 01	
TRUE ANOMALY -	1.409898373D 02	

S-IVB LUNAR-IMPACT TRAJECTORY (CONTINUED)

16 APRIL 1972 G.M.T. = 23 HR 49 MIN 6.000000 SEC

TIME = 23.81833

PTC COMMANDED

PARAMETER	GEOCENTRIC	SELENOCENTRIC
X -	6.5604093190 03	-1.0899524350 05
Y -	4.7133821320 04	-2.5910306200 05
Z -	2.8988121670 04	-1.3018792290 05
|R| -	5.5722053780 04	3.0977936390 05
XD -	-8.5338175220-01	1.4891064540-01
YD -	3.0760769690 00	2.6898922010 00
ZD -	1.5483802770 00	1.4438353070 00
|V| -	3.5479559490 00	3.0565265960 00
DECLINATION -	3.1349297100 01	-4.2000407420 00
LONGITUDE -	-1.2040215890 02	2.9152987790 00
SEMI-MAJOR AXIS -	2.3190154670 05	
ECCENTRICITY -	0.9718642500 00	
INCLINATION -	3.2493735910 01	
RIGHT ASC. OF NODE -	-2.4883435120 01	
ARG. OF PERIFOCUS -	-3.7881393830 01	
TRUE ANOMALY -	1.4231392890 02	

S-IVB LUNAR-IMPACT TRAJECTORY (CONTINUED)

17 APRIL 1972 G.M.T. = 0 HR 0 MIN 0.0 SEC

TIME = 24.00000

PARAMETER	GEOCENTRIC	SELENOCENTRIC
X -	5.9992888350 03	-1.0890066280 05
Y -	4.9122916400 04	-2.5736598450 05
Z -	2.9986887060 04	-1.2925724520 05
|R| -	5.7864201140 04	3.0790264540 05
XD -	-8.6229591180-01	1.4061224460-01
YD -	3.0075948270 00	2.6230861670 00
ZD -	1.5064706190 00	1.4027974060 00
|V| -	3.4725544790 00	2.9779512090 00
DECLINATION -	3.1215270680 01	-4.1900270940 00
LONGITUDE -	-1.2217368170 02	2.7027947470 00
SEMI-MAJOR AXIS -	2.3194013380 05	
ECCENTRICITY -	0.9718707190 00	
INCLINATION -	3.2492328740 01	
RIGHT ASC. OF NODE -	-2.4880529670 01	
ARG. OF PERIFOCUS -	-3.7884680770 01	
TRUE ANOMALY -	1.4314689710 02	

S-IVB LUNAR-IMPACT TRAJECTORY (CONTINUED)

17 APRIL 1972 G.M.T. = 6 HR 0 MIN 0.0 SEC

TIME = 30.00000

PARAMETER	GEOCENTRIC	SELENOCENTRIC
X -	-1.301660584D 04	-1.060495295D 05
Y -	9.991718150D 04	-2.142756996D 05
Z -	5.425119685D 04	-1.069209003D 05
|R| -	1.144380511D 05	2.619019945D 05
XD -	-8.560408630D-01	1.650940336D-01
YD -	1.931358717D 00	1.632679372D 00
ZD -	8.869839106D-01	8.121541614D-01
|V| -	2.291220834D 00	1.804281461D 00
DECLINATION -	2.829953227D 01	-4.036728871D 00
LONGITUDE -	1.619652068D 02	-3.771669265D 00
SEMI-MAJOR AXIS -	2.322081100D 05	
ECCENTRICITY -	0.971915036D 00	
INCLINATION -	3.248796203D 01	
RIGHT ASC. OF NODE -	-2.483623312D 01	
ARG. OF PERIFOCUS -	-3.792327302D 01	
TRUE ANOMALY -	1.559618543D 02	

S-IVB LUNAR-IMPACT TRAJECTORY (CONTINUED)

17 APRIL 1972 G.M.T. = 12 HR 0 MIN 0.0 SEC

TIME = 36.00000

PARAMETER	GEOCENTRIC	SELENOCENTRIC
X -	-3.0697854590 04	-1.0151425380 05
Y -	1.3670440610 05	-1.8397814360 05
Z -	7.0776450550 04	-9.1700238890 04
|R| -	1.5697[illegible]668D 05	2.2926411420 05
XD -	-7.8[illegible]3326084D-01	2.5293576870-01
YD -	1.5184680200 00	1.2463539880 00
ZD -	6.6798101870-01	6.2200[illegible]0649D-01
|V| -	1.8341177940 00	1.4157[illegible]5670 00
DECLINATION -	2.6801460830 01	-3.[illegible]49282790 00
LONGITUDE -	7.6952590000 01	-9.4664659200 00
SEMI-MAJOR AXIS -	2.3246075380 05	
ECCENTRICITY -	0.9719968870 00	
INCLINATION -	3.2495167710 01	
RIGHT ASC. OF NODE -	-2.4858410330 01	
ARG. OF PERIFOCUS -	-3.7919139910 01	
TRUE ANOMALY -	1.6085199410 02	

S-IVB LUNAR-IMPACT TRAJECTORY (CONTINUED)

17 APRIL 1972 G.M.T. = 18 HR 0 MIN 0.0 SEC

TIME = 42.00000

PARAMETER	GEOCENTRIC	SELENOCENTRIC
X -	-4.689142077D 04	-9.523007399D 04
Y -	1.666699695D 05	-1.592748258D 05
Z -	8.375247871D 04	-7.940651674D 04
|R| -	1.923334649D 05	2.018480385D 05
XD -	-7.189448543D-01	3.263851414D-01
YD -	1.273053839D 00	1.057979819D 00
ZD -	5.427648924D-01	5.255328867D-01
|V| -	1.559532465D 00	1.225574712D 00
DECLINATION -	2.581469928D 01	-3.980727570D 00
LONGITUDE -	-1.023647627D 01	-1.463371654D 01
SEMI-MAJOR AXIS -	2.327234468D 05	
ECCENTRICITY -	0.972203934D 00	
INCLINATION -	3.252064831D 01	
RIGHT ASC. OF NODE -	-2.492700021D 01	
ARG. OF PERIFOCUS -	-3.791069720D 01	
TRUE ANOMALY -	1.638141815D 02	

S-IVB LUNAR-IMPACT TRAJECTORY (CONTINUED)

17 APRIL 1972 G.M.T. = 21 HR 3 MIN 59.000000 SEC

TIME = 45.06639

CCS DOWNLINK SIGNAL LOST

PARAMETER	GEOCENTRIC	SELENOCENTRIC
X -	-5.4668695510 04	-9.1447204760 04
Y -	1.8018899910 05	-1.4796857860 05
Z -	8.9476665300 04	-7.3791873180 04
|R| -	2.0847737340 05	1.8395113440 05
XD -	-6.9049733080-01	3.5841579480-01
YD -	1.1788794480 00	9.9305802900-01
ZD -	4.9571816950-01	4.9309223980-01
|V| -	1.4533684390 00	1.1652322030 00
DECLINATION -	2.5416653960 01	-3.9773622340 00
LONGITUDE -	-5.5194219690 01	-1.7113548040 01
SEMI-MAJOR AXIS -	2.3267426080 05	
ECCENTRICITY -	0.9723584000 00	
INCLINATION -	3.2540807760 01	
RIGHT ASC. OF NODE -	-2.4977612700 01	
ARG. OF PERIFOCUS -	-3.7902797500 01	
TRUE ANOMALY -	1.6497150210 02	

S-IVB LUNAR-IMPACT TRAJECTORY (CONTINUED)

18 APRIL 1972 G.M.T. = 0 HR 0 MIN 0.0 SEC

TIME = 48.00000

PARAMETER	GEOCENTRIC	SELENOCENTRIC
X -	-6.182630332D 04	-8.7513460520 04
Y -	1.9222134120 05	-1.3775080350 05
Z -	9.4505180310 04	-6.8717614580 04
|R| -	2.2294117040 05	1.7707625470 05
XD -	-6.652795940-01	3.8608362080-01
YD -	1.1015598300 00	9.4374838630-01
ZD -	4.5751696570-01	4.6879324080-01
|V| -	1.3657791640 00	1.1222694340 00
DECLINATION -	2.5081524600 01	-3.9750258650 00
LONGITUDE -	-9.836c594210 01	-1.9398326970 01
SEMI-MAJOR AXIS -	2.3303216520 05	
ECCENTRICITY -	0.9725452010 00	
INCLINATION -	3.2565992770 01	
RIGHT ASC. OF NODE -	-2.5038419490 01	
ARG. OF PERIFOCUS -	-3.7891782320 01	
TRUE ANOMALY -	1.6593596540 02	

S-IVB LUNAR-IMPACT TRAJECTORY (CONTINUED)

18 APRIL 1972 G.M.T. = 6 HR 0 MIN 0.0 SEC

TIME = 54.00000

PARAMETER	GEOCENTRIC	SELENOCENTRIC
X -	-7.568075787D 04	-7.8629077430 04
Y -	2.145495581D 05	-1.182128440D 05
Z -	1.036714927D 05	-5.9002871390 04
|R| -	2.500137363D 05	1.5374702110 05
XD -	-6.184817527D-01	4.3494912810-01
YD -	9.711666842D-01	8.7059736300-01
ZD -	3.939876146D-01	4.3342481100-01
|V| -	1.216926722D 00	1.0653532650 00
DECLINATION -	2.449835693D 01	-9.9700294180 00
LONGITUDE -	1.729869596D 02	-2.3835338560 01
SEMI-MAJOR AXIS -	2.334098033D 05	
ECCENTRICITY -	0.973080135D 00	
INCLINATION -	3.264158541D 01	
RIGHT ASC. OF NODE -	-2.5211715920 01	
ARG. OF PERIFOCUS -	-3.7853410550 01	
TRUE ANOMALY -	1.6760878790 02	

S-IVB LUNAR-IMPACT TRAJECTORY (CONTINUED)

18 APRIL 1972 G.M.T. = 12 HR 0 MIN 0.0 SEC

TIME = 60.00000

PARAMETER	GEOCENTRIC	SELENOCENTRIC
X -	-8.8578208390 04	-6.8785122060 04
Y -	2.3436306670 05	-9.9955484980 04
Z -	1.1162272430 05	-4.9899651070 04
|R| -	2.7428412010 05	1.3119629210 05
XD -	-5.7635005720-01	4.7526360250-01
YD -	8.6701242160-01	8.2343353700-01
ZD -	3.4409099320-01	4.1123533210-01
|V| -	1.0964891880 00	1.0358729560 00
DECLINATION -	2.4014191900 01	-3.9609794370 00
LONGITUDE -	8.4014854580 01	-2.7993344440 01
SEMI-MAJOR AXIS -	2.3389323780 05	
ECCENTRICITY -	0.9739023480 00	
INCLINATION -	3.2765634850 01	
RIGHT ASC. OF NODE -	-2.5479889930 01	
ARG. OF PERIFOCUS -	-3.7779667210 01	
TRUE ANOMALY -	1.6901935230 02	

S-IVB LUNAR-IMPACT TRAJECTORY (CONTINUED)

18 APRIL 1972 G.M.T. = 18 HR 0 MIN 0.0 SEC

TIME = 66.00000

PARAMETER	GEOCENTRIC	SELENOCENTRIC
X -	-1.005999780D 05	-5.814586875D 04
Y -	2.521381515D 05	-8.251025978D 04
Z -	1.186047200D 05	-4.117299563D 04
|R| -	2.962449704D 05	1.090142202D 05
XD -	-5.371211358D-01	5.088865349D-01
YD -	7.815432371D-01	7.944831304D-01
ZD -	3.037729046D-01	3.980710325D-01
|V| -	9.957845769D-01	1.024026121D 00
DECLINATION -	2.3600806210 01	-3.943256181D 00
LONGITUDE -	-5.184413883D 00	-3.190184253D 01
SEMI-MAJOR AXIS -	2.345482391D 05	
ECCENTRICITY -	0.975172141D 00	
INCLINATION -	3.297409640D 01	
RIGHT ASC. OF NODE -	-2.590645331D 01	
ARG. OF PERIFOCUS -	-3.763883443D 01	
TRUE ANOMALY -	1.702802098D 02	

S-IVB LUNAR-IMPACT TRAJECTORY (CONTINUED)

19 APRIL 1972 G.M.T. = 0 HR 0 MIN 0.0 SEC

TIME = 72.00000

PARAMETER	GEOCENTRIC	SELENOCENTRIC
X -	-1.117900368D 05	-4.683591370D 04
Y -	2.682334277D 05	-6.553100718D 04
Z -	1.248002836D 05	-3.265306046D 04
|R| -	3.162614341D 05	8.691454413D 04
XD -	-4.990051600D-01	5.377171675D-01
YD -	7.111353211D-01	7.799155118D-01
ZD -	2.710875367D-01	3.918941003D-01
|V| -	9.100593647D-01	1.025177518D 00
DECLINATION -	2.324177095D 01	-3.909790440D 00
LONGITUDE -	-9.455763616D 01	-3.556895450D 01
SEMI-MAJOR AXIS -	2.355098823D 05	
ECCENTRICITY -	0.977191717D 00	
INCLINATION -	3.335004632D 01	
RIGHT ASC. OF NODE -	-2.663216925D 01	
ARG. OF PERIFOCUS -	-3.735723030D 01	
TRUE ANOMALY -	1.714841738D 02	

S-IVB LUNAR-IMPACT TRAJECTORY (CONTINUED)

19 APRIL 1972 G.M.T. = 6 HR 0 MIN 0.0 SEC

TIME = 78.00000

PARAMETER	GEOCENTRIC	SELENOCENTRIC
X -	-1.221461250D 05	-3.493123116D 04
Y -	2.829651680D 05	-4.871822856D 04
Z -	1.303688286D 05	-2.419530401D 04
|R| -	3.346415896D 05	6.464572146D 04
XD -	-4.592718962D-01	5.646068993D-01
YD -	6.556403818D-01	7.793879198D-01
ZD -	2.458776638D-01	3.924623652D-01
|V| -	6.374071951D-01	1.039352293D 00
DECLINATION -	2.292821265D 01	-3.845145385D 00
LONGITUDE -	1.759194956D 02	-3.896239206D 01
SEMI-MAJOR AXIS -	2.371200507D 05	
ECCENTRICITY -	0.980604937D 00	
INCLINATION -	3.413907165D 01	
RIGHT ASC. OF NODE -	-2.804540124D 01	
ARG. OF PERIFOCUS -	-3.671936489D 01	
TRUE ANOMALY -	1.727572817D 02	

S-IVB LUNAR-IMPACT TRAJECTORY (CONTINUED)

19 APRIL 1972 G.M.T. = 12 HR 0 MIN 0.0 SEC

TIME = 84.00000

PARAMETER	GEOCENTRIC	SELENOCENTRIC
X -	-1.3157196770 05	-2.2410963400 04
Y -	2.9671202990 05	-3.1714100040 04
Z -	1.3549895250 05	-1.5627749470 04
|R| -	3.5172315440 05	4.1860028200 04
XD -	-4.1082877800-01	5.9677878510-01
YD -	6.2253555120-01	8.0019651230-01
ZD -	2.3175098450-01	4.0330598910-01
|V| -	7.8105013680-01	1.0766220770 00
DECLINATION -	2.2658803440 01	-3.7007454710 00
LONGITUDE -	8.6239012710 01	-4.1915550260 01
SEMI-MAJOR AXIS -	2.4062478810 05	
ECCENTRICITY -	0.9870082770 00	
INCLINATION -	3.0521625360 01	
RIGHT ASC. OF NODE -	-3.1763238030 01	
ARG. OF PERIFOCUS -	-3.4705411220 01	
TRUE ANOMALY -	1.7442486340 02	

S-IVB LUNAR-IMPACT TRAJECTORY (CONTINUED)

19 APRIL 1972 G.M.T. = 18 HR 0 MIN 0.0 SEC

TIME = 90.00000

PARAMETER	GEOCENTRIC	SELENOCENTRIC
X -	-1.395871964D 05	-8.867336131D 03
Y -	3.103739577D 05	-1.364338971D 04
Z -	1.406305574D 05	-6.528725523D 03
|R| -	3.682301868D 05	1.753271174D 04
XD -	-3.114211017D-01	6.766262964D-01
YD -	6.745247036D-01	9.048767772D-01
ZD -	2.587398040D-01	4.543866177D-01
|V| -	7.867102164D-01	1.217822781D 00
DECLINATION -	2.245194778D 01	-3.156677663D 00
LONGITUDE -	-3.706177937D 00	-4.321279024D 01
SEMI-MAJOR AXIS -		-5.307069255D 03
ECCENTRICITY -		1.032043697D 00
INCLINATION -		1.506891593D 01
RIGHT ASC. OF NODE -		-3.139279645D 01
ARG. OF PERIFOCUS -		1.495497977D 02
TRUE ANOMALY -		-1.617782512D 02

S-IVB LUNAR-IMPACT TRAJECTORY (CONTINUED)

19 APRIL 1972 G.M.T. = 21 HR 1 MIN 54.935756 SEC

TIME = 93.03193

LUNAR IMPACT

PARAMETER	GEOCENTRIC	SELENOCENTRIC
X -	-1.417434352D 05	-2.938967724D 02
Y -	3.197530611D 05	-1.607077291D 03
Z -	1.443683875D 05	-5.906953561D 02
|R| -	3.783853230D 05	1.738090228D 03
XD -	1.710275061D-01	1.147985589D 00
YD -	1.828971547D 00	2.085434855D 00
ZD -	7.406843170D-01	9.481506090D-01
|V| -	1.980656605D 00	2.562401027D 00
DECLINATION -	2.242894690D 01	2.242506619D 00
LONGITUDE -	-4.961764766D 01	-2.448562544D 01
SEMI-MAJOR AXIS -		-5.304142556D 03
ECCENTRICITY -		1.032787511D 00
INCLINATION -		1.491223556D 01
RIGHT ASC. OF NODE -		-3.294131047D 01
ARG. OF PERIFOCUS -		1.492179481D 02
TRUE ANOMALY -		-1.404720417D 02
HEADING -		1.048359751D 02
IMPACT ANGLE -		1.709820366D 01

THIS PAGE LEFT BLANK INTENTIONALLY